Inorg. Chem. **1989**, *28*, 567–578

Contribution from the Department of Chemistry,
University of Houston, University Park, Houston, Texas 77204-5641

Oxidation–Reduction of Carbonylcobalt Cation–Anion Pairs in Coupling to Dimeric Cobalt Carbonyls

K. Y. Lee and J. K. Kochi*

Received July 29, 1988

The carbonylcobalt cation $Co(CO)_3(PPh_3)_2^+$ reacts with the anionic $Co(CO)_3PPh_3^-$ upon mixing to afford quantitative yields of the dimeric $Co_2(CO)_6(PPh_3)_2$. The same coupling occurs with the analogous Bu_3P-substituted cation–anion pair to produce $Co_2(CO)_6(PBu_3)_2$, but at a significantly attenuated rate. Cross couplings of the substitution-inert $Co(CO)_3P_2^+$ and $Co(CO)_3P'^-$, as well as the reverse phosphine combination, afford mixtures of $Co_2(CO)_6P_2$, $Co_2(CO)_6PP'$ and $Co_2(CO)_6P'_2$ diagnostic of extensive ligand (P,P′) scramblings. Facile ligand exchange of reactive intermediates is also indicated by the production of only $Co_2(CO)_6(PBu_3)_2$ from $Co(CO)_3(PPh_3)_2^+$ and $Co(CO)_3PPh_3^-$ when carried out in the presence of added PBu_3—without materially affecting the coupling rate. The marked solvent and salt effects together with the observation of characteristic charge-transfer absorption bands point to the contact ion pairs $[Co(CO)_3P_2^+][Co(CO)_3P'^-]$ as critically involved in the rate-limiting activation process. A general mechanistic formulation is presented in Scheme II, in which the contact ion pair evolves into the radical pair consisting of the 19-electron $Co(CO)_3P_2^\bullet$ and the 17-electron $Co(CO)_3P'^\bullet$. The behavior of these carbonylcobalt radicals is independently established in the preparative and transient electrochemistry of their precursors $Co(CO)_3P_2^+$ and $Co(CO)_3P'^-$ in reduction (E_c) and oxidation (E_a), respectively. Indeed the reactivity patterns in ion-pair annihilation parallel the differences in the redox potentials $\mathcal{F}(E_c - E_a)$ as a direct measure of the driving force for electron transfer. Cyclic voltammetry is shown to be a particularly useful probe to demonstrate (i) the rapid dimerization rates of the 17-electron radicals to afford dicobalt carbonyls and (ii) the facile exchange of phosphine ligands between $Co(CO)_3P^\bullet$ and $Co(CO)_3P'^\bullet$ via the highly labile 19-electron intermediates $Co(CO)_3PP'^\bullet$. Although the electron-transfer mechanism in Scheme II accounts for all the experimental observations relating to ion-pair annihilation, the possibility of alternative nonradical pathways previously proposed is also discussed.

Introduction

The ready disproportionation of dicobalt octacarbonyl induced by Lewis bases has been known for more than 3 decades,[1] but the process still presents an intriguing mechanistic knot. Thus with nitrogen- and oxygen-centered bases (B), the disproportionation of $Co_2(CO)_8$ usually affords a Co(II)/Co(−I) salt with the general stoichiometry[2-4]

$$3Co_2(CO)_8 + 12B \rightarrow 2[CoB_6^{2+}][Co(CO)_4^-]_2 + 8CO \quad (1)$$

On the other hand, with phosphorus-centered bases (P), especially in polar solvents, dicobalt octacarbonyl disproportionates even at room temperature to produce the Co(I)/Co(−I) salt with a simpler stoichiometry,[5-9] i.e.

$$Co_2(CO)_8 + 2P \rightarrow [Co(CO)_3P_2^+][Co(CO)_4^-] + CO \quad (2)$$

Interestingly, the same phosphines react with dicobalt octacarbonyl in nonpolar solvents at higher temperatures by effecting an overall ligand substitution,[9,10] i.e.

$$Co_2(CO)_8 + 2P \rightarrow Co_2(CO)_6P_2 + 2CO \quad (3)$$

It is known that this disubstitution product can also be obtained by heating the Co(I)/Co(−I) salt,[10,11] i.e.

$$[Co(CO)_3P_2^+][Co(CO)_4^-] \rightarrow Co_2(CO)_6P_2 + CO \quad (4)$$

Such an ion-pair annihilation can be formally considered as the microscopic reverse of the disproportionation in eq 2. As such, it is possible to envisage a reversible disproportionation that is induced by carbon monoxide, i.e.

$$Co_2(CO)_8 + CO \rightleftharpoons [Co(CO)_5^+][Co(CO)_4^-] \quad (5)$$

Although this interchange of dicobalt octacarbonyl with its ion pair remains as yet hypothetical[12] (owing to the unknown pentacarbonylcobalt(I) cation), its viability can be established with the corresponding manganese carbonyls.[13] Indeed among the various carbonylcobalt(I) cations extant, the bis(phosphine)-substituted derivative $Co(CO)_3P_2^+$ is the most common—only a few examples of the mono(phosphine)-substituted cation $Co(CO)_4P^+$ having been reported.[14,15] Accordingly the previous mechanistic investigations of cobalt-centered ion pairs[16,17] have focused on the annihilation of the disproportionation ion pair $[Co(CO)_3P_2^+][Co(CO)_4^-]$ that is obtained directly from dicobalt octacarbonyl by treatment with phosphines.[18,19] However we believe that this problem can be approached more generally from a consideration of carbonylcobalt cations as electrophilic electron acceptors and carbonylcobalt anions as nucleophilic electron donors in a manner similar to that recently established in the annihilation of carbonylmanganese ion pairs.[20] Since phosphine ligands are known to strongly modulate the redox properties of carbonylmetals,[21] we have selected for our studies the substituted carbo-

---

(1) (a) Ellis, J. E. *J. Organomet. Chem.* **1975**, *86*, 1. (b) Manuel, T. A. *Adv. Organomet. Chem.* **1965**, *3*, 181. (c) Kemmitt, R. D. W.; Russell, D. R. In *Comprehensive Organometallic Chemistry*; Wilkinson, G., Ed.; Pergamon: Oxford, England, 1982; Vol. 5, p 1. (d) Pidcock, A. L. In *Transition Metal Complexes of Phosphorus, Arsenic and Antimony Ligands*; McAuliffe, C. A., Ed.; John Wiley & Sons: New York, 1973; p 88.

(2) Wender, I.; Sternberg, H. W.; Orchin, M. *J. Am. Chem. Soc.* **1952**, *74*, 1216.

(3) Tucchi, E. R.; Gwynn, G. H. *J. Am. Chem. Soc.* **1964**, *86*, 4838.

(4) (a) Hieber, W.; Sedlmeier, J.; Abeck, W. *Chem. Ber.* **1953**, *86*, 700. (b) Hieber, W.; Sedlmeier, J. *Chem. Ber.* **1954**, *87*, 25. (c) Hieber, W.; Wiesboeck, R. *Chem. Ber.* **1958**, *91*, 1146.

(5) (a) Sacco, A.; Freni, M. *J. Inorg. Nucl. Chem.* **1958**, *8*, 566. (b) Sacco, A.; Freni, M. *Ann. Chim.* **1958**, *48*, 218.

(6) Vohler, O. *Chem. Ber.* **1958**, *91*, 1235.

(7) Attali, S.; Poilblanc, R. *Inorg. Chim. Acta.* **1972**, *6*, 475.

(8) Hieber, W.; Freyer, F. *Chem. Ber.* **1960**, *93*, 462.

(9) Hieber, W.; Freyer, F. *Chem. Ber.* **1958**, *91*, 1230.

(10) McCleverty, J. A.; Davison, A.; Wilkinson, G. *J. Chem. Soc. A* **1969**, 2610.

(11) Manning, A. R. *J. Chem. Soc. A* **1968**, 1135.

(12) However, see: Metlin, S.; Wender, I.; Sternberg, H. W. *Nature* **1959**, *183*, 457.

(13) Kruck, T.; Höfler, M. *Chem. Ber.* **1964**, *97*, 2289.

(14) Hieber, W.; Duchatsch, H. *Chem. Ber.* **1965**, *98*, 1745.

(15) For partial characterization of the piperidine derivative see Wender et al.[2]

(16) (a) Mirbach, M. F.; Mirbach, M. J.; Wegman, R. W. *Organometallics* **1984**, *3*, 900. (b) Compare ref 11 and: King, R. B. *Inorg. Chem.* **1963**, *2*, 936.

(17) Atwood, J. D. *Inorg. Chem.* **1987**, *26*, 2918.

(18) Heck, R. F. *J. Am. Chem. Soc.* **1963**, *85*, 657.

(19) (a) Absi-Halabi, M.; Atwood, J. D.; Forbus, N. P.; Brown, T. L. *J. Am. Chem. Soc.* **1980**, *102*, 6248. (b) See also: Sweany, R. L.; Brown, T. L. *Inorg. Chem.* **1977**, *16*, 415.

(20) Lee, K. Y.; Kuchynka, D. J.; Kochi, J. K. *Organometallics* **1987**, *6*, 1886.

(21) For leading references, see: (a) Kuchynka, D. J.; Amatore, C.; Kochi, J. K. *Inorg. Chem.* **1986**, *25*, 4087. (b) Kuchynka, D. J.; Amatore, C.; Kochi, J. K. *J. Organomet. Chem.* **1987**, *328*, 133. (c) Hershberger, J. W.; Kochi, J. K. *Polyhedron* **1983**, *2*, 929.

0020-1669/89/1328-0567$01.50/0

Table I. Characteristic Carbonyl Stretching Bands in the Infrared Spectra of Carbonylcobalt Species[a]

cobalt carbonyl		
P	X^-	carbonyl band (ν_{CO}), cm^{-1}
		$Co(CO)_3P_2^+X^-$ [b]
PPh_3	PF_6^-	2078 (vw), 2015 (sh), 2004 (s)
$P(p\text{-}CH_3C_6H_4)_3$	PF_6^-	2073 (vw), 2009 (sh), 2001 (s)
$P(n\text{-}Bu)_3$	ClO_4^-	2065 (vw), 1994 (sh), 1986 (s)
		$Co(CO)_3P^-Y^+$ [c]
CO	PPN^+	1886
PPh_3	Na^+	1931 (m), 1856 (s), 1810 (m)
PPh_3	PPN^+	1928 (m), 1843 (s)
$P(n\text{-}Bu)_3$	Na^+	1929 (w), 1841 (s), 1795 (w)
$P(n\text{-}Bu)_3$	PPN^+	1918 (m), 1826 (s)
		$Co_2(CO)_6P_2$ [d]
$[PPh_3]_2$		1943[e]
$[P(n\text{-}Bu)_3]_2$		1963 (vw), 1944 (s)
$[(PPh_3)(PBu_3)]$		1970 (vw), 1950 (s)
$[CO]_2$		2072 (s), 2041 (s), 2021 (sh), 1847 (m)[f]

[a] In THF solution, unless indicated otherwise. [b] Compare with ref 25 and 35. [c] PPN = $Ph_3P{=}N{=}PPh_3^+$. Compare with ref 17, 26–28. [d] Compare with ref 11 and 19b. [e] KBr disk. [f] In CH_2Cl_2.

nylcobalt(I) cations $Co(CO)_3P_2^+$ and carbonylcobaltate(−I) anions $Co(CO)_3P^-$ that contain PPh_3 and PBu_3 as the prototypical aryl- and alkylphosphines, respectively.[22,23]

Results

I. Preparation of Carbonylcobalt Cations and Anions. The disubstituted carbonylcobalt(I) cation $Co(CO)_3(PPh_3)_2^+$ was obtained from the disproportionation of dicobalt octacarbonyl with triphenylphosphine in the presence of the appropriate ferrocenium (Fc^+) salt, e.g.[24]

$$Co_2(CO)_8 + 2Fc^+PF_6^- \xrightarrow{PPh_3} 2Co(CO)_3(PPh_3)_2^+PF_6^- + 2Fc + 2CO \quad (6)$$

The corresponding tri-*n*-butylphosphine analogue was obtained as the perchlorate salt from the carbonylation of $Co(ClO_4)_2$ in isopropyl alcohol in the presence of excess $n\text{-}Bu_3P$.[25] Each cation was identified by its distinctive carbonyl stretching band in the infrared spectrum (Table I).

The monosubstituted carbonylcobaltate(−I) anion $Co(CO)_3P^-$ with P = PPh_3 or $P(n\text{-}Bu)_3$ was prepared from the substituted carbonylcobalt dimer by reduction with 1% sodium amalgam.[17,26] The corresponding PPN^+ salt was prepared by metathesis with bis(triphenylphosphoranylidene)ammonium chloride, e.g.[27]

$$Co_2(CO)_6(PPh_3)_2 \xrightarrow{Na(Hg)} 2Na^+Co(CO)_3PPh_3^- \xrightarrow{PPN^+Cl^-} PPN^+Co(CO)_3PPh_3^- \quad (7)$$

The carbonyl bands of these carbonylcobaltates are included in Table I together with those of the parent $Co(CO)_4^-$ prepared from the disproportionation of dicobalt octacarbonyl with alkali in THF.[28]

II. Coupling of Carbonylcobalt(I) Cations with Carbonylcobaltate(−I) Anions. The interactions of the phosphine-substituted carbonylcobalt cations and anions can be considered in two ways. Thus the use of the same phosphine as the ligand in the cation as well as in the anion leads to a symmetrical dicobalt carbonyl, hereafter referred to as the *homo dimer*. On the other hand, the use of different phosphine ligands in the carbonylcobalt cation and anion could lead to an unsymmetrical *cross dimer* as described below. [Note the counterions are not indicated hereafter (see Table I).]

A. Homo Dimers from Carbonylcobalt Ion Pairs. When equimolar amounts of $Co(CO)_3(PPh_3)_2^+$ and $Co(CO)_3PPh_3^-$ in tetrahydrofuran (THF) solutions were mixed at 25 °C, a quantitative reaction resulted immediately (<5 min)[29] according to the stoichiometry in eq 8. The homo dimer $Co_2(CO)_6(PPh_3)_2$

$$Co(CO)_3(PPh_3)_2^+ + Co(CO)_3PPh_3^- \xrightarrow[THF]{fast} Co_2(CO)_6(PPh_3)_2 + PPh_3 \quad (8)$$

largely precipitated as a red solid in 98% yield, and it was characterized by its distinctive carbonyl band at ν_{CO} = 1943 cm^{-1} in the IR spectrum.[11] An equivalent amount of free triphenylphosphine was also extracted from the reaction mixture in accord with the stoichiometry in eq 8. When the corresponding ion pair that contained only tri-*n*-butylphosphine as the ligand was treated in a similar manner, high yields (93%) of the homo dimer $Co_2(CO)_6(PBu_3)_2$ were obtained. However this coupling occurred at a significantly diminished rate (~30 min),[29] as judged by the slow disappearance of the pair of carbonyl bands (simultaneously) at 1986 and 1841 cm^{-1} for the cation and anion, respectively. The more soluble homo dimer $Co_2(CO)_6(PBu_3)_2$ was extracted in 93% yield, and it was identified by its characteristic IR spectrum.[11]

$$Co(CO)_3(PBu_3)_2^+ + Co(CO)_3PBu_3^- \xrightarrow[THF]{slow} Co_2(CO)_6(PBu_3)_2 + PBu_3 \quad (9)$$

No other carbonyl-containing product (< 5%) was observed.

B. Cross Dimers from Carbonylcobalt Ion Pairs. When $Co(CO)_3(PPh_3)_2^+$ was treated with an equimolar amount of $Co(CO)_3PBu_3^-$ in THF solution at 25 °C, the initial IR spectrum of the reaction mixture that was recorded within 5 min showed no carbonyl band of either starting material. Immediate separation of the red solid yielded the homo dimer $Co_2(CO)_6(PPh_3)_2$ in 35% yield, and the thin-layer chromatography (TLC) of the mother liquor afforded a pure crystalline sample of the other homo dimer $Co_2(CO)_6(PBu_3)_2$ in 28% yield. The remaining carbonyl-containing product was identified as the cross dimer $Co_2(CO)_6(PPh_3)(PBu_3)$ in 29% yield by the comparison of its IR spectrum with that of an authentic sample (see Experimental Section), i.e.

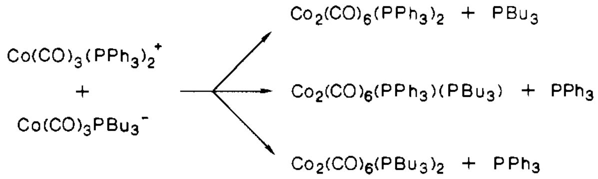

(10)

The alternative ion-pair combination of $Co(CO)_3(PBu_3)_2^+$ and $Co(CO)_3PPh_3^-$ required a significantly longer time (~30 min) for completion. TLC of the red solution yielded only the homo dimer $Co_2(CO)_6(PBu_3)_2$ in 54% yield together with the cross dimer $Co_2(CO)_6(PPh_3)(PBu_3)$ in 26% yield. There was no evidence of the other homo dimer $Co_2(CO)_6(PPh_3)_2$, either by isolation as an insoluble red precipitate (vide supra) or from its IR spectrum (Table I).

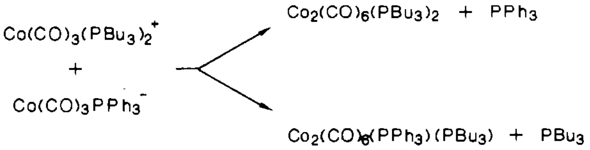

(11)

By way of comparison, the ion pair from the disproportionation of dicobalt octacarbonyl with tri-*n*-butylphosphine in eq 2 with P = PBu_3 was also treated in THF under the same reaction

---

(22) Compare the reactivities reported by King, (King, R. B. *Inorg. Chem.* **1963**, *2*, 936) Manning,[11] and McCleverty et al.[10]

(23) See: Arabi, M. S.; Maisonnat, A.; Attali, S.; Poilblanc, R. *J. Organomet. Chem.* **1974**, *67*, 109.

(24) (a) Schumann, H. *J. Organomet. Chem.* **1985**, *290*, C34. (b) Hendrickson, D. N.; Sohn, Y. S.; Gray, H. B. *Inorg. Chem.* **1971**, *10*, 1559.

(25) Rigo, P.; Bressan, M.; Morvillo, A. *J. Organomet. Chem.* **1976**, *105*, 263.

(26) Hieber, W.; Lindner, E. *Chem. Ber.* **1961**, *94*, 1417.

(27) Ruff, J. K.; Schlientz, W. J. *Inorg. Synth.* **1979**, *15*, 87.

(28) Edgell, W. F., Lyford, J. IV *Inorg. Chem.* **1970**, *9*, 1932.

(29) Since the course of ion-pair annihilation was followed by conventional IR analysis, all conversions (rates) hereinafter refer to the time required for completion after the first measurement (~5 min). These qualitative indications were sufficient to indicate the reactivity patterns of ion pairs for purposes of this study.

conditions. However at these temperatures less than 5% of the homo dimer was produced over a 60-h period, i.e.

$$\mathrm{Co(CO)_3(PBu_3)_2^+ + Co(CO)_4^- \xrightarrow[\text{slow}]{\text{very}} Co_2(CO)_6(PBu_3)_2 + CO} \quad (12)$$

C. Effect of Added Phosphine on the Ion-Pair Coupling. The rate of the homo coupling of $Co(CO)_3(PPh_3)_2^+$ and $Co(CO)_3(PPh_3)^-$ in eq 8 was materially unaffected when the THF solution contained up to 15 equiv of added tri-*n*-butylphosphine.[29] However we could find no evidence of $Co_2(CO)_6(PPh_3)_2$ (<5%), the only carbonyl-containing product being the replaced homo dimer $Co_2(CO)_6(PBu_3)_2$ isolated in 84% yield, i.e.

$$\mathrm{Co(CO)_3(PPh_3)_2^+ + Co(CO)_3PPh_3^- \xrightarrow{PBu_3\ (excess)} Co_2(CO)_6(PBu_3)_2 + 3PPh_3} \quad (13)$$

Control experiments established that neither the carbonylcobalt cation nor the carbonylcobalt anion underwent prior ligand substitution by the added PBu_3 under the reaction conditions. Moreover the homo dimer $Co_2(CO)_6(PPh_3)_2$ and the cross dimer $Co_2(CO)_6(PPh_3)(PBu_3)$ were not subject to subsequent ligand substitution by tributylphosphine to yield the homo dimer in eq 13.

D. Effect of Solvent Polarity on Ion-Pair Annihilation. When the homo coupling of $Co(CO)_3(PPh_3)_2^+$ and $Co(CO)_3PPh_3^-$ in eq 8 was carried out in a more polar solvent such as acetonitrile, the formation of $Co_2(CO)_6(PPh_3)_2$ in 84% yield was noticeably retarded.[29] Moreover the solvent effect was unmistakable in the homo coupling of the tributylphosphine-substituted ion pair (eq 9), which was essentially inert in acetonitrile for periods exceeding 10 h. The crossed ion pair in eq 11 was similarly unreactive in acetonitrile, i.e.

$$\mathrm{Co(CO)_3(PBu_3)_2^+ + Co(CO)_3PPh_3^- \xrightarrow[MeCN]{} no\ reaction} \quad (14)$$

with only a small amount (~10%) of the anion $Co(CO)_3PPh_3^-$ diminished after 10 h.[30] (The concentration of the more stable cation $Co(CO)_3(PBu_3)_2^+$ was unchanged.)

E. Inhibitory Effects of Added Salts on the Ion-Pair Coupling. The homo coupling of $Co(CO)_3(PPh_3)_2^+$ and $Co(CO)_3PPh_3^-$ in THF solution was visibly retarded by the presence of 0.3 M tetra-*n*-butylammonium perchlorate (TBAP), but the yield of the homo dimer $Co_2(CO)_6(PPh_3)_2$ was unaffected. The negative salt effect in tetrahydrofuran was dramatic in the case of the less reactive $Co(CO)_3(PBu_3)_2^+/Co(CO)_3PBu_3^-$ pair of ions. Thus the presence of 0.3 M TBAP was sufficient to retard the conversion in eq 9 to less than 5% over a 10-h period.

$$\mathrm{Co(CO)_3(PBu_3)_2^+ + Co(CO)_3PBu_3^- \xrightarrow{TBAP} no\ reaction} \quad (15)$$

Similarly, the cross-coupling pair that consisted of $Co(CO)_3(PBu_3)_2^+$ and $Co(CO)_3PPh_3^-$ yielded less than 5% $Co_2(CO)_6(PBu_3)_2$ in THF solution over a 10-h period when 0.3 M TBAP was added. IR analysis indicated that the concentration of the reactant ion-pair was essentially undiminished.

III. Spectral Study of Ion Pairs from Carbonylcobalt Cations and Carbonylcobaltate Anions. The ion-pair interactions of carbonylcobalt(I) cations with carbonylcobaltate(−I) anions was apparent in both their electronic and infrared spectra taken in solution and in the solid state.

A. The electronic spectra of both precursor salts $Co(CO)_3(PBu_3)_2^+ClO_4^-$ and $Co(CO)_4^-PPN^+$ showed essentially no absorptions beyond $\lambda > 350$ nm (Figure 1). However the crystalline carbonylcobalt salt $[Co(CO)_3(PBu_3)_2^+][Co(CO)_4^-]$ obtained by disproportionation (eq 2, P = *n*-Bu_3P) was a bright yellow color, which appeared in the diffuse reflectance spectrum as a broad absorption with a shoulder (λ_{max} ~ 400 nm) tailing out to beyond 500 nm (see inset). By comparison, the color of a solution of 3.5×10^{-3} M $[Co(CO)_3(PBu_3)_2^+][Co(CO)_4^-]$ dissolved in tetrahydrofuran was also yellow, and it showed the same absorption band, as illustrated in Figure 1. Moreover this band appeared when the separate ions $Co(CO)_3(PBu_3)_2^+$ and $Co(CO)_4^-$ as the ClO_4^- and PPN^+ salts, respectively, were mixed in tetrahydrofuran. As such, the new spectral band with λ_{max} ~ 400 nm was assigned to the charge-transfer absorption ($h\nu_{CT}$) of the contact ion pair, i.e.[31]

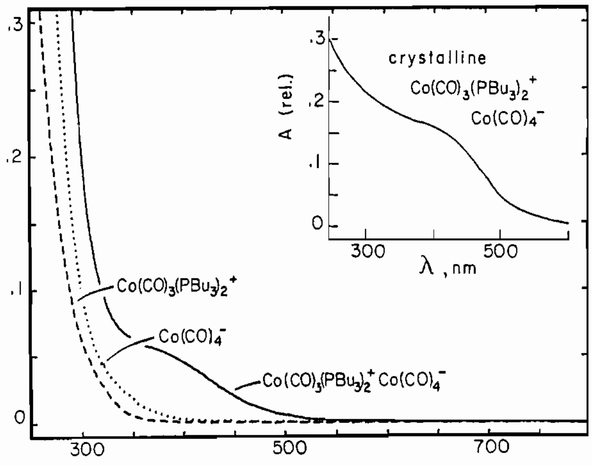

Figure 1. Absorption spectra of 3.5×10^{-3} M solutions of $Co(CO)_3(PBu_3)_2^+$ (- -), $Co(CO)_4^-$ (···), and $[Co(CO)_3(PBu_3)_2^+][Co(CO)_4^-]$ in THF (—). Inset: Solid-state reflectance spectrum of crystalline $[Co(CO)_3(PBu_3)_2^+][Co(CO)_4^-]$ after dilution with SiO_2.

Table II. Ion-Pair Associations from the Charge-Transfer Spectra of $[Co(CO)_3(PBu_3)_2^+][Co(CO)_4^-]$ in Solution and in the Solid State[a]

solvent	dielectric const[b]	λ_{CT},[c] nm
tetrahydrofuran	7.58	~400
dichloromethane	9.08	*d*
chlorobenzene	5.62	418[e]
acetonitrile	37.5	*d*
p-chlorotoluene	6.08	439[e]
diethyl ether	4.34	464[f]
solid state (crystallin)		~400[g]

[a] In 3.5×10^{-3} M solution at 25 °C, unless indicated otherwise. [b] From ref 32. [c] At absorption maximum. [d] CT band too weak to measure. [e] At −40 °C. [f] At −78 °C. [g] Diffuse reflectance spectrum diluted (10%) in silica gel (400 mesh).

$$\mathrm{[Co(CO)_3(PBu_3)_2^+][Co(CO)_4^-] \xrightarrow{h\nu_{CT}} [Co(CO)_3(PBu_3)_2^{\bullet}][Co(CO)_4^{\bullet}]} \quad (16)$$

In order to confirm this assignment, we examined the effects of solvent polarity and added salts on the behavior of the disproportionation salt $[Co(CO)_3(PBu_3)_2^+][Co(CO)_4^-]$ in solution.

Solvent polarity strongly affected the nature of $[Co(CO)_3(PBu_3)_2^+][Co(CO)_4^-]$ in solution as evidenced by the color change from orange in diethyl ether, to yellow-orange in chlorobenzene, to yellow in tetrahydrofuran, to pale yellow in dichloromethane and finally to colorless in acetonitrile. The corresponding shift in the electronic absorption bands in Figure 2A paralleled the trend in the dielectric constant (Table II).[32] As such, the complete bleaching of the color was consistent with the disappearance of the contact ion pair (and its associated charge-transfer band at ~400 nm) by stabilization of the separated ions in polar solvents such as acetonitrile, i.e.

$$\mathrm{[Co(CO)_3(PBu_3)_2^+][Co(CO)_4^-] \underset{}{\overset{MeCN}{\rightleftharpoons}} Co(CO)_3(PBu_3)_2^+ + Co(CO)_4^-} \quad (17)$$

By the same token, we attribute the spectral red shift observed

---

[30] Note that carbonylcobaltate anions unlike their cationic counterparts are not persistent indefinitely in solution.

[31] Bockman, T. M., Kochi, J. K. *J. Am. Chem. Soc.* **1988**, *110*, 1294.

[32] Dean, J. A., Ed. *Lange's Handbook of Chemistry*, 12th ed.; McGraw Hill: New York, 1979.

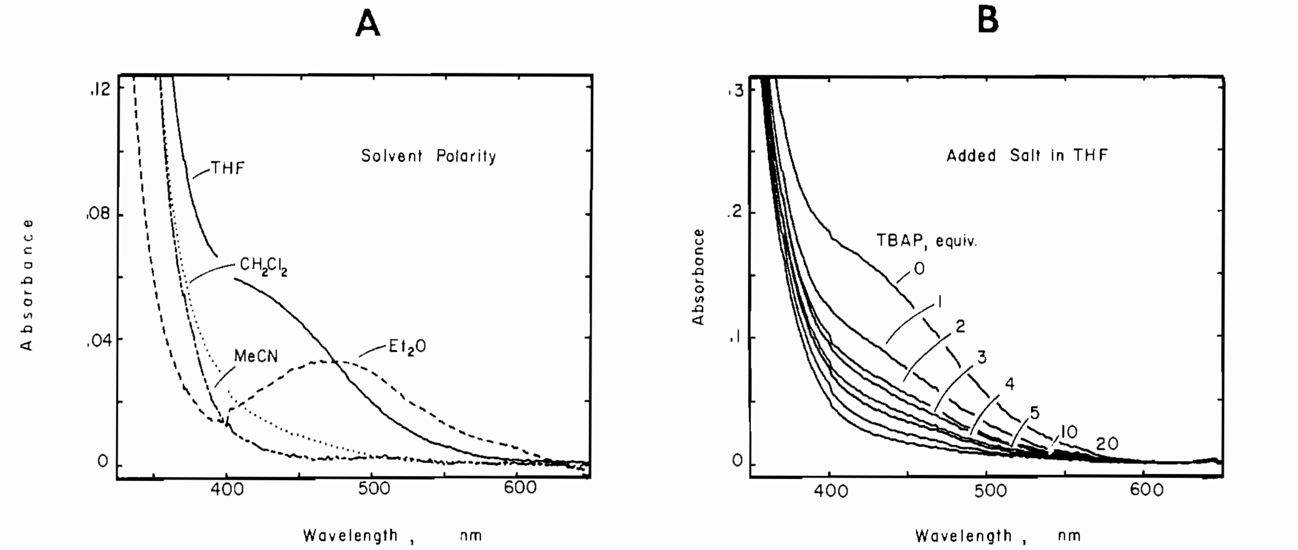

Figure 2. Charge-transfer absorption spectrum of 3.5 × 10^{-3} M $[Co(CO)_3(PBu_3)_2^+][Co(CO)_4^-]$: (A) solvent effect, with THF (—), CH_2Cl_2 (···), MeCN (– – –), and Et_2O (- -); (B) salt effect, with TBAP added being (top to bottom) 0, 1, 2, 3, 4, 5, 10, and 20 equiv relative to 1 × 10^{-2} M $[Co(CO)_3(PBu_3)_2^+][Co(CO)_4^-]$ in THF.

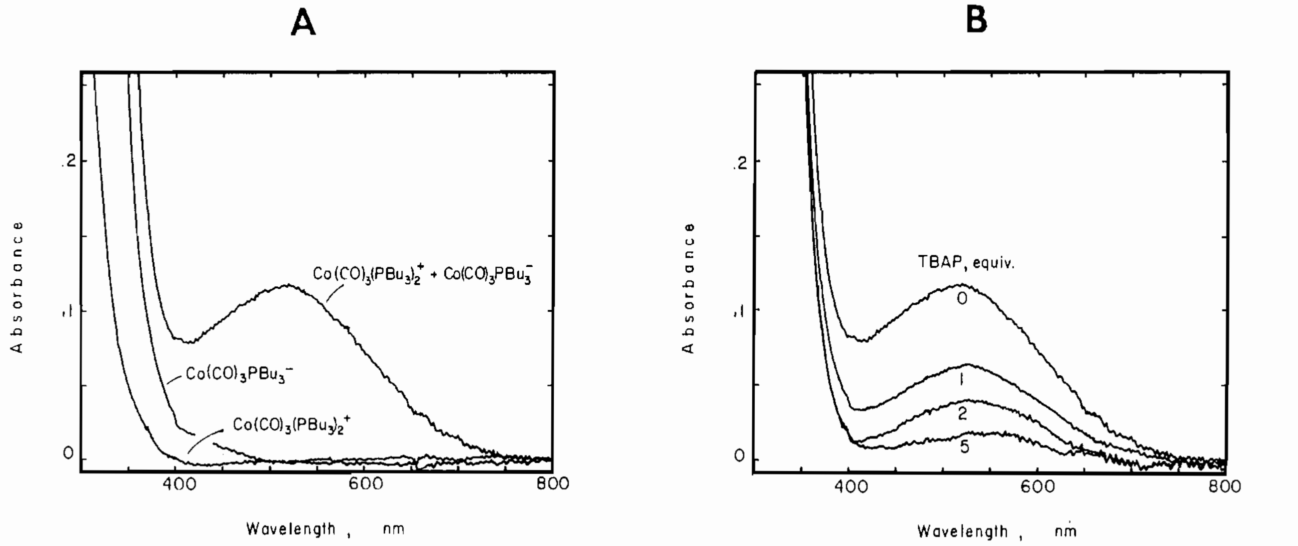

Figure 3. Left: contact ion pairs observed by the appearance of the charge-transfer absorption band upon (a) mixing equimolar amounts of 2.5 × 10^{-4} M $Co(CO)_3(PBu_3)_2^+ClO_4^-$ and $Co(CO)_3PBu_3^-PPN^+$ at −78 °C, in comparison with (b) 2.5 × 10^{-4} M $Co(CO)_3PBu_3^-PPN^+$ at −78 °C and (c) 2.5 × 10^{-4} M $Co(CO)_3(PBu_3)_2^+ClO_4^-$ at 25 °C in THF. Right: Salt effect on the solution prepared for part a with added TBAP being (top to bottom) 0, 1.0, 2.0, and 5.0 equiv relative to the ion pair.

in diethyl ether (Table II) to the interionic contraction induced by this least polar solvent.[33]

Added salts like tetra-*n*-butylammonium perchlorate (TBAP) strongly perturbed the intensity of the color of $[Co(CO)_3(PBu_3)_2^+][Co(CO)_4^-]$ in THF solution. Thus Figure 2B shows the pronounced hypochromic effect on only the charge-transfer band with $\lambda_{max} \sim 400$ nm by incremental amounts of added TBAP. Indeed the presence of merely 1 equiv of TBAP was sufficient to reduce the concentration of the contact ion pair by half. We conclude that ion-pair exchange in eq 18 effectively

$$[Co(CO)_3(PBu_3)_2^+][Co(CO)_4^-] + [Bu_4N^+][ClO_4^-] \rightleftharpoons [Co(CO)_3(PBu_3)_2^+][ClO_4^-] + [Bu_4N^+][Co(CO)_4^-] \quad (18)$$

separated the carbonylcobalt cation from the carbonylcobaltate anion in the contact ion pair.[31] As such, the disappearance of the CT band in Figure 2B was reminiscent of the situation achieved with highly polar solvents.

It is important to emphasize that the equimolar combination of salts in eq 18 was equivalent to the mixture of the separate carbonylcobalt salts such as $[Co(CO)_3(PBu_3)_2^+][ClO_4^-]$ and $[n\text{-}Bu_4N^+][Co(CO)_4^-]$ that were employed above in ion-pair annihilation (eq 12). These expectations are borne out in Figure 3, which illustrates the presence of the well-resolved charge-transfer band with $\lambda_{CT} = 520$ nm of $[Co(CO)_3(PBu_3)_2^+][Co(CO)_3PBu_3^-]$. This contact ion pair was instantaneously generated upon mixing the separate carbonylcobalt salts that were individually transparent beyond $\lambda > 400$ nm (Figure 3A). Moreover the suppression of the CT absorption band by added TBAP in Figure 3B was the same as that presented for disproportionation salt in Figure 2B. Indeed the generality of the negative salt effect on such charge-transfer spectra emphasized its validity as the experimental criterion for the existence of contact ion pairs.[34]

B. The infrared spectra of the disproportionation salts $[Co(CO)_3(PBu_3)_2^+][Co(CO)_4^-]$ and $[Co(CO)_3(PPh_3)_2^+][Co(CO)_4^-]$ consisted by and large of the spectral composite of the individual ionic components. Thus the IR absorptions of the carbonylcobalt cation in the carbonyl region occurred at $\nu_{CO} = 2000\text{–}2800$ cm^{-1} and those for the carbonylcobaltate anionic moiety at ν_{CO} =

---

[33] Compare Davis, K. M. C. *Mol. Assoc.* **1975**, *1*, 151.

[34] Szwarc, M., Ed. Ions and Ion Pairs in Organic Reactions; Wiley: New York: 1972, Vol. 1; 1974, Vol. 2.

Table III. Ion-Pair Distortions from the Carbonyl IR Bands of $[Co(CO)_3P_2^+][Co(CO)_4^-]$ in Solution and in the Solid State[a]

	carbonyl band,[b] (ν_{CO}), cm^{-1}	
medium	$Co(CO)_3(PPh_3)_2^+$	$Co(CO)_4^-$
acetonitrile	2010 (m)	1893 (s)
dichloromethane	2010 (m)	1889 (s)
tetrahydrofuran	2076 (vw), 2014 (sh), 2006 (m)	1886 (s)
Nujol mull	2071 (vs), 2014 (s), 2001 (s)	1897 (sh), 1887 (s), 1873 (s)
KBr disk	2072 (vw), 2014 (s), 2001 (s)	1895 (s), 1885 (s), 1871 (sh)

	carbonyl band,[b] (ν_{CO}), cm^{-1}	
medium	$Co(CO)_3(P\text{-}n\text{-}Bu_3)_2^+$	$Co(CO)_4^-$
acetonitrile	2065 (vw), 1996 (br)	1893 (s)
dichloromethane	2068 (vw), 1995 (br)	1889 (br)
tetrahydrofuran	2066 (vw), 1996 (s), 1989 (s)	1887 (s)
chlorobenzene	2067 (vw), 1996 (s), 1989 (s)	1900 (sh), 1887 (s), 1875 (sh)
Nujol mull	2066 (vw), 1997 (s), 1983 (s)	1882 (br)
KBr disk	2063 (vw), 2000 (s), 1981 (s)	1979 (br)

[a] In 5×10^{-3} M solutions at 20 °C. [b] Key: vw, very weak; m, medium; s, strong; br, broad absorption bands.

1870–1900 cm^{-1} (Table III). However a closer examination of the IR absorption bands revealed a systematic variation of ν_{CO} with solvent polarity. Thus the carbonyl band of $Co(CO)_3(PPh_3)_2^+$ in acetonitrile and dichloromethane consisted of a single band with $\nu_{CO} = 2010$ cm^{-1} for the E′ mode in D_{3h} symmetry. This band in a less polar THF medium was split into two components appearing as a shoulder and a weak A_1' band that are forbidden in D_{3h} symmetry. Moreover the salt in either a KBr disk or a Nujol mull also showed well-resolved splittings into three distinct bands (Table III) symptomatic of cation distortion to C_{2v} symmetry.[35] A change in the carbonyl bands of the carbonylcobaltate anion also accompanied the transition from solution to the crystal. Thus the carbonyl band of $Co(CO)_4^-$ in either acetonitrile, dichloromethane, or tetrahydrofuran consisted of a single band at $\nu_{CO} \sim 1890$ cm^{-1}, as expected for the tetrahedral anion with T_d symmetry. However in the crystal of $[Co(CO)_3(PPh_3)_2^+][Co(CO)_4^-]$ this triply degenerate band was split into three distinct components (Table III) diagnostic of a configurational change to C_{3v} symmetry.[36,37] Owing to an adventitious overlap with the cation absorptions, the weak A_1 band that was forbidden in T_d symmetry was not identified.[31] Such simultaneous distortions of both the carbonylcobalt cation and carbonylcobaltate anion (as indicated by infrared studies) thus mirror the solvent-induced changes in the amount of ion pairing (as deduced from the charge-transfer absorptions). Both spectroscopic probes point to the relevance of the intimate molecular interactions extant in contact ion pairs. Furthermore the existence of the charge-transfer absorption bands (Table II) was characteristic of important electron-donor–electron-acceptor contributions to the contact ion pair.[38] Accordingly, we focused our attention on the redox behavior of carbonylcobalt cations and carbonylcobaltate anions with electrochemical probes.

Table IV. Preparative Electroreduction of Carbonylcobalt(I) Cations[a]

P in $Co(CO)_3P_2^+$	E,[b] V vs SCE	solvent	n[c]	products: type, mmol (%)
PPh_3	−0.70	THF	0.87	$Co_2(CO)_6P_2$, 0.135 (87); PPh_3, 0.27
PPh_3	−0.70	MeCN	1.14	$Co_2(CO)_6P_2$, 0.129 (83); PPh_3, 0.28
$P(n\text{-}Bu)_3$	−1.35	THF	1.71	$Co(CO)_3P^-$, 0.15 (100)[d]

[a] With $Co(CO)_3(PPh_3)_2^+PF_6^-$ or $Co(CO)_3(PBu_3)_2^+ClO_4^-$ (0.31 mmol) in 30 mL of MeCN (THF) containing 0.3 (0.1) M TBAP at 23 °C. [b] Constant potential of bulk reduction. [c] Electron uptake per mole of $Co(CO)_3P_2^+$. [d] Only carbonyl-containing product was observed. Free PBu_3 was detected but not quantified.

IV. Redox Behaviors of Carbonylcobalt Cations and Carbonylcobaltate Anions. As electron acceptors, the carbonylcobalt(I) cations were generally reduced at negative potentials of ~−0.7 V vs SCE. Analogously carbonylcobaltate anions as electron donors were generally oxidized at the more positive potentials of ~−0.3 V. The redox stoichiometries of carbonylcobalt cations and anions as well as their transient electrochemical behavior are described individually below.

A. Preparative electroreductions of carbonylcobalt cations such as $Co(CO)_3(PPh_3)_2^+$ were carried out potentiostatically at a platinum electrode in THF solutions containing 0.3 M tetra-*n*-butylammonium perchlorate (TBAP) as supporting electrolyte. The uptake of 0.87 faraday of charge/mol of $Co(CO)_3(PPh_3)_2^+$ resulted in the corresponding dicobalt carbonyl according to the stoichiometry in eq 19. The liberated triphenylphosphine was

$$Co(CO)_3(PPh_3)_2^+ + e^- \xrightarrow{[-0.7\ V]} {}^1\!/\!_2Co_2(CO)_6(PPh_3)_2 + PPh_3 \tag{19}$$

separated by thin-layer chromatography and quantitatively determined by ^1H NMR analysis. Essentially the same results were obtained in the cathodic reduction of $Co(CO)_3(PPh_3)_2^+$ in acetonitrile (Table IV). By contrast, a more negative potential of −1.35 V was required to effect the potentiostatic reduction of $Co(CO)_3(PBu_3)_2^+$ at the same platinum electrode. From the uptake of 1.71 faraday of charge/mol of carbonylcobalt cation to produce 1 equiv of the anionic $Co(CO)_3PBu_3^-$, we deduced the redox stoichiometry to be

$$Co(CO)_3(PBu_3)_2^+ + 2e^- \xrightarrow{[-1.35\ V]} Co(CO)_3PBu_3^- + PBu_3 \tag{20}$$

Infrared analysis of the carbonyl region (Table I) indicated that the carbonylcobaltate(−I) anion $Co(CO)_3PBu_3^-$ was the sole carbonyl-containing product of the electroreduction in eq 20.

B. Preparative electrooxidations of carbonylcobaltate(−I) anions such as $Co(CO)_3PPh_3^-$ were carried out at a constant potential of −0.15 V in THF solution containing 0.3 M TBAP. The requirement of 0.93 faraday of charge/mol of $Co(CO)_3PPh_3^-$ resulted in the formation of the corresponding carbonylcobalt dimer according to the stoichiometry

$$Co(CO)_3PPh_3^- - e^- \xrightarrow{[-0.2\ V]} {}^1\!/\!_2Co_2(CO)_6(PPh_3)_2 \tag{21}$$

Essentially the same results were obtained when the electrooxidation of $Co(CO)_3PPh_3^-$ was carried out in the presence of a 3-fold excess of triphenylphosphine (Table V). The electrooxidation of the parent carbonylcobaltate $Co(CO)_4^-$ under the same conditions afforded a complex mixture of products owing to the further reaction of the dimeric $Co_2(CO)_8$ with the solvent. However the anodic oxidation of $Co(CO)_4^-$ in the presence of 2 equiv of added triphenylphosphine at a constant potential of 0.3 V required 1.07 faraday of charge to produce the phosphine-substituted carbonylcobalt dimer in 80% yield according to the stoichiometry

$$Co(CO)_4^- + PPh_3 - e^- \xrightarrow{[-0.3\ V]} {}^1\!/\!_2Co_2(CO)_6(PPh_3)_2 + CO \tag{22}$$

Small but discrete amounts of the carbonylcobalt cation $Co(CO)_3(PPh_3)_2^+$ were also produced (Table V). Importantly the amount of $Co(CO)_3(PPh_3)_2^+$ rose with increasing concentrations of added PPh_3. The concomitant decrease in the amount of the dimeric $Co_2(CO)_6(PPh_3)_2$ also coincided with the increasing

---

(35) Hieber, W.; Duchatsch, H. *Chem. Ber.* **1965**, *98*, 2530.

(36) Cf.: Edgell, W. F.; Lyford, J., IV; Barbetta, A.; Jose, C. I. *J. Am. Chem. Soc.* **1971**, *93*, 6403. Edgell, W. F. In ref 34: 1972, Vol. 1, p 153. See also: Schramm, C.; Zink, J. I. *J. Am. Chem. Soc.* **1980**, *19*, 2854.

(37) For the related $Mn(CO)_5^-$, see: Darensbourg, M. Y.; Darensbourg, D. J.; Burns, D.; Drew, D. A. *J. Am. Chem. Soc.* **1976**, *98*, 3127. Pribula, C. D.; Brown, T. L. *J. Organomet. Chem.* **1974**, *71*, 415.

(38) (a) For example, the charge-transfer band of $[Co(CO)_3(PPh_3)_2^+][Co(CO)_4^-]$ severely overlapped with the absorption band of $Co(CO)_3(PPh_3)_2^+$ owing to the limited value of $(E_c - E_a)$ in Table VI compared to that of $[Co(CO)_3(PBu_3)_2^+][Co(CO)_4^-]$ shown in Figure 1. (b) For the photoinduced electron transfer by irradiation of the CT band, see: Vogler, A.; Kunkely, H. *Organometallics* **1988**, *7*, 1449.

Table V. Preparative Electrooxidation of Carbonylcobaltate(−I) Anions[a]

L in $Co(CO)_3L^-$	E,[b] V vs SCE	mmol of PPh_3[c]	n[d]	amt, mmol (%)[e] $Co_2(CO)_6(PPh_3)_2$	amt, mmol (%)[e] $Co(CO)_3(PPh_3)_2^+$	mater bal,[f] %
PPh_3	−0.15	0	0.93	0.070 (90)	0	90
PPh_3	−0.15	0.47 (0.42)	0.98	0.076 (98)	0	98
CO	+0.30	0.31 (0.14)	1.07	0.062 (80)	0.018 (12)	92
CO	+0.30	0.62 (0.43)	1.33	0.037 (48)	0.061 (39)	87
CO	+0.30	0.93 (0.64)	1.45	0.032 (41)	0.082 (53)	94

[a] In 30 mL of THF containing 1.55×10^{-3} mol $Na^+Co(CO)_3PPh_3^-$ or $PPN^+Co(CO)_4^-$ and 0.3 M TBAP. [b] Constant electrode potential. [c] Added triphenylphosphine (amount of reisolated PPh_3 in parentheses). [d] Faradays of charge required per mole of carbonylcobaltate added. [e] By IR analysis. [f] Material balance of carbonylcobalt species.

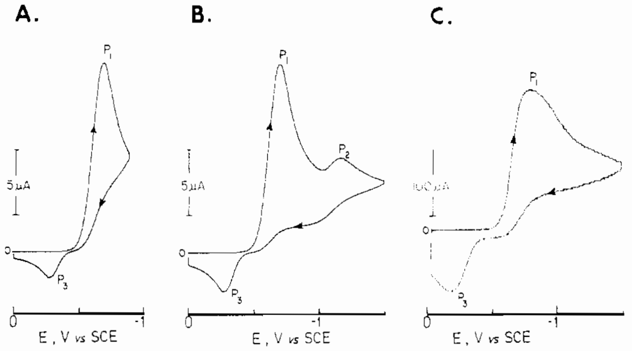

Figure 4. Initial negative-scan cyclic voltammogram of 5×10^{-3} M $Co(CO)_3(PPh_3)_2^+$ containing 0.3 M TBAP. Switching potential at (A) −0.9 V or (B) −1.5 V at $v = 0.5$ V s^{-1}. (C) Switching potential under the same conditions as in part B, but at $v = 100$ V s^{-1}.

electrochemical requirement of n (Table V). Control experiments established that no phosphine-induced ligand substitution of $Co(CO)_4^-$ occurred in the absence of anodic current [certainly within the time period (2 h) of the electrolysis].

C. Transient electrochemical methods such as cyclic voltammetry have proven to be invaluable probes for the elucidation of the dynamic processes accompanying the oxidation–reduction of carbonylmetal cations and anions.[39] As applied to this study, the initial negative-scan cyclic voltammograms of $Co(CO)_3(PPh_3)_2^+$ and $Co(CO)_3(PBu_3)_2^+$ readily revealed the mechanistic basis for their different stoichiometries in preparative electroreductions described by eq 19 and 20, respectively.

Thus the cyclic voltammogram of 5×10^{-3} M $Co(CO)_3(PPh_3)_2^+$ at a sweep rate $v = 0.5$ V s^{-1} in THF (Figure 4A) showed a cathodic peak P_1 with $E_p = -0.69$ V vs SCE (Table VI) that corresponded to an uptake of 0.95 electron by calibration relative to a ferrocene standard.[40] Such a cathodic current led to two reduction products. The presence of the carbonylcobaltate $Co(CO)_3PPh_3^-$ in the cyclic voltammogram was indicated by the anodic peak P_3 with $E_p = -0.27$ V when the initial CV scan was reversed at −0.9 V. By comparison with the CV behavior of an authentic sample of $Co(CO)_3PPh_3^-$, the electrode process for P_3 was

$$Co(CO)_3PPh_3^- - e^- \xrightarrow{[P_3]} \tfrac{1}{2}Co_2(CO)_6(PPh_3)_2 \qquad (23)$$

The dimeric $Co_2(CO)_6(PPh_3)_2$ was also formed as the other product of the cathodic reduction of $Co(CO)_3(PPh_3)_2^+$, and its presence was indicated by the appearance of the cathodic peak P_2 with $E_p = -1.15$ V when the initial CV scan was carried out to a more negative potential of −1.5 V in Figure 4B.[41] By comparison with the CV behavior of an authentic sample of $Co_2(CO)_6(PPh_3)_2$, the electrode process for P_2 was described as

Table VI. Electrochemical Parameters for the Cyclic Voltammetry of Carbonylcobalt Species[a]

P in $Co(CO)_3P_2^+$	electroreduction E_c[b] THF	electroreduction E_c[b] MeCN	P in $Co(CO)_3P^-$	electrooxidation E_a[c] THF	electrooxidation E_a[c] MeCN
PPh_3[d]	−0.69	−0.81	PPh_3	−0.27	−0.28
PBu_3	−1.36	−1.42	PBu_3	−0.35	−0.39
PEt_3	−1.20	−1.36	PEt_3	−0.40	−0.44
PPh_2Me	−0.87	−0.95	PPh_2Me	−0.29	−0.33
$PPhMe_2$	−1.00	−1.11	$PPhMe_2$	−0.35	−0.39
			$P(p\text{-}MeC_6H_4)_3$	−0.28	−0.31
			CO	+0.28	

P in $Co_2(CO)_6P_2$	electroreduction E_c[b] THF	electroreduction E_c[b] MeCN	P in $Co_2(CO)_6P_2$	electroreduction E_c[b] THF	electroreduction E_c[b] MeCN
PPh_3	−1.15	−1.03	PPh_2Me	−1.21	−1.15
PBu_3	−1.66	*e*	$PPhMe_2$	−1.25	*e*

[a] With 5×10^{-3} M carbonylcobalt species at $v = 0.5$ V s^{-1} in THF and MeCN containing 0.3 and 0.1 M TBAP respectively, at 23 °C under an argon atmosphere. [b] Irreversible cathodic wave in V vs SCE. [c] Irreversible anodic wave. [d] For comparison, for $Co(CO)_4PPh_3^+BF_4^-$, $E_c = -0.30$ V in CH_2Cl_2/0.1 M TBAP at 0.5 V s^{-1}. [e] Not observed.

$$Co_2(CO)_6(PPh_3)_2 + 2e^- \xrightarrow{[P_2]} 2Co(CO)_3PPh_3^- \qquad (24)$$

The relative amounts of the reduction products $Co(CO)_3PPh_3^-$ and $Co_2(CO)_6(PPh_3)_2$ were indicated by the peak current ratio i_2/i_3. This ratio decreased monotonically as the CV scans of $Co(CO)_3(PPh_3)_2^+$ were increased, until P_2 disappeared at $v = 100$ V s^{-1} as shown in Figure 4C.[42,44] Accordingly the electrode process for P_1 represented a composite reduction,[45] i.e.

$$Co(CO)_3(PPh_3)_2^+ + xe^- \xrightarrow{[P_1]} [Co(CO)_3PPh_3^- + Co_2(CO)_6(PPh_3)_2] + PPh_3 \qquad (25)$$

By way of contrast, the cyclic voltammogram of the *n*-butyl analogue $Co(CO)_3(PBu_3)_2^+$ at the same sweep rate ($v = 0.5$ V s^{-1}) shows in Figure 5A the cathodic peak P_1 at the significantly more negative potential of $E_p = -1.36$ V. The cathodic wave P_1 corresponded to the uptake of 1.3 electron, which accounted for the observation of the carbonylcobaltate $Co(CO)_3PBu_3^-$ by its anodic wave P_3 at $E_p = -0.35$ V; i.e.

$$Co(CO)_3(PBu_3)_2^+ + 2e^- \xrightarrow{[P_1]} Co(CO)_3PBu_3^- \qquad (26)$$

It is noteworthy that the cathodic peak P_2 at $E_p = -1.66$ V due to the dimeric $Co_2(CO)_6(PBu_3)_2$ was missing, and it was not evident even when the return CV scan was reversed at −1.0 V

---

(39) (a) Kochi, J. K. *J. Organomet. Chem.* **1986**, *300*, 139. (b) Narayanan, B. A.; Amatore, C.; Kochi, J. K. *Organometallics* **1986**, *5*, 926. See also ref 21a,b.

(40) Gagne, R. R.; Koval, C. A.; Lisensky, G. C. *Inorg. Chem.* **1980**, *19*, 2854.

(41) It is noteworthy that the cyclic voltammetry of $Co(CO)_3(PPh_3)_2^+$ in acetonitrile differed from that obtained at the same scan rate in THF (Figure 4) in the significantly smaller cathodic wave P_2 and the barely perceptible $Co_2(CO)_6(PPh_3)_2$.

(42) Note the CV wave broadening at $V = 100$ V s^{-1} (Figure 4C) was due to uncompensated *iR* drop and nonfaradaic charging current.[43]

(43) Wipf, D. O.; Kristensen, E. W.; Deakin, M. R.; Wightman, R. M. *Anal. Chem.* **1988**, *60*, 306.

(44) A similar effect was noted at high concentrations of $PPh_3 > 30$ equiv at which $i_2/i_3 \rightarrow 0$ at $v = 0.5$ V s^{-1}.

(45) The electron requirement in eq 25 is $1 < x < 2$, which depends on the relative amounts of $Co(CO)_3PPh_3^-$ ($x = 2$) and $^1/_2Co_2(CO)_6(PPh_3)_2$ ($x = 1$) formed.

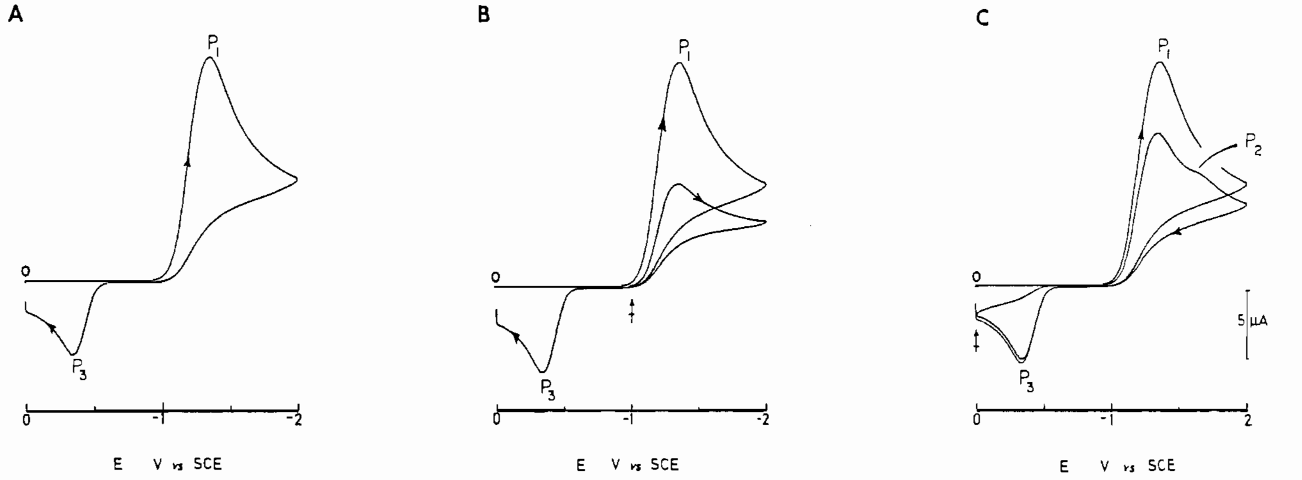

Figure 5. Initial negative-scan cyclic voltammogram of (A) 5×10^{-3} M $Co(CO)_3(PBu_3)_2^+$ in THF containing 0.3 M TBAP at $v = 0.5$ V s^{-1} and voltammograms under the same conditions as above, except that the reverse scan was reswitched at (B) −1.0 V or (C) 0 V vs SCE, as indicated by the arrow (↑).

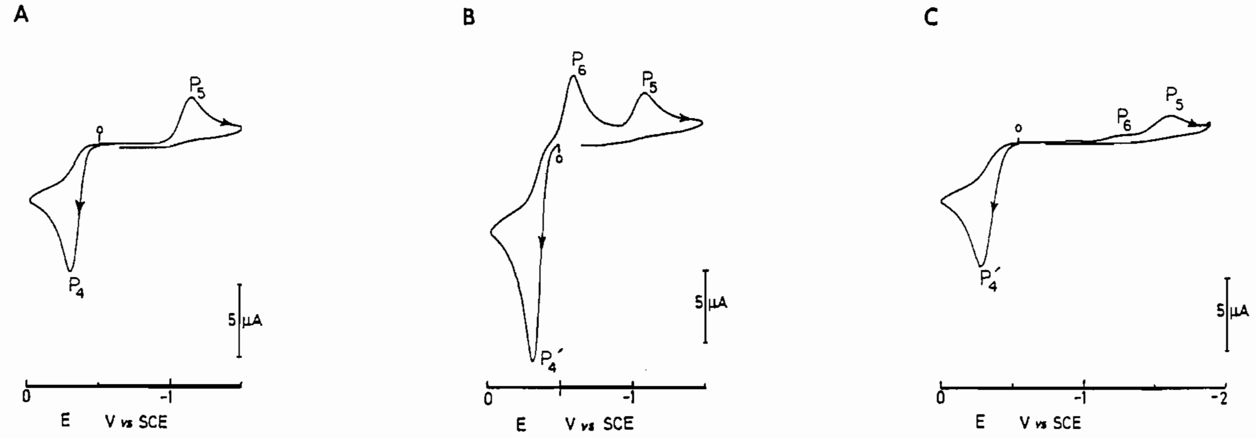

Figure 6. Initial positive scan cyclic voltammograms of 5×10^{-3} M $Co(CO)_3PPh_3^-$ in THF containing 0.3 M TBAP at $v = 0.5$ V s^{-1} in the presence of (A) no added phosphine, (B) 6 equiv of added PPh_3, or (C) 1 equiv of added PBu_3, relative to carbonylcobaltate.

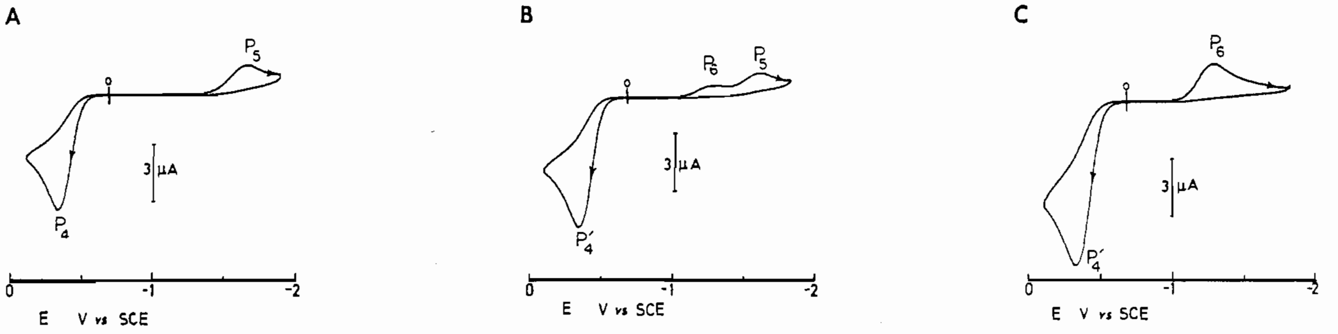

Figure 7. Initial positive scan cyclic voltammograms of 5×10^{-3} M $Co(CO)_3PBu_3^-$ in THF containing 0.3 M TBAP at $v = 0.5$ V s^{-1} in the presence of (A) 0, (B) 1, or (C) 10 equiv of added PBu_3.

(Figure 5B). It only became (barely) observable when the return CV scan was reversed at the more positive potential of 0 V (Figure 5C), i.e., after the anodic peak P_3 had been scanned through (see eq 23). We thus concluded that the reductive dimerization of $Co(CO)_3(PBu_3)_2^+$ to $Co_2(CO)_6(PBu_3)_2$ on the *CV time scale* was much less important than that observed with the phenyl analogue $Co(CO)_3(PPh_3)_2^+$ in eq 25.[46]

D. Cyclic voltammetry of the carbonylcobaltate anion $Co(CO)_3PPh_3^-$ in THF on the initial positive scan showed an anodic wave P_4 with $E_p = -0.27$ V vs SCE at $v = 0.5$ V s^{-1}. The anodic wave in Figure 6A was the same as P_3 observed from $Co(CO)_3(PPh_3)_2^+$ in Figure 4 and corresponded to the oxidative dimerization of the carbonylcobaltate; i.e.

$$Co(CO)_3PPh_3^- - e^- \xrightarrow{[P_4]} \tfrac{1}{2}Co_2(CO)_6(PPh_3)_2 \qquad (27)$$

as shown by the presence of the cathodic wave P_5 with $E_p = -1.15$ V on the return negative scan. [By comparison with the CV behavior of $Co_2(CO)_6(PPh_3)_2$, the cathodic wave P_5 was the same as P_2 in Figure 4B.]

An additional cathodic wave P_6 with $E_p = -0.69$ V was observed when the free ligand triphenylphosphine was present (Figure 6B). The new cathodic wave corresponded to P_1 in Figure 4A. As such, the increase in $Co(CO)_3(PPh_3)_2^+$ in the presence of added PPh_3, was associated with the electrode process

$$Co(CO)_3PPh_3^- - 2e^- \xrightarrow[Ph_3P]{[P_4']} Co(CO)_3(PPh_3)_2^+ \qquad (28)$$

---

(46) For the relevance of the time scale in cyclic voltammetry vis à vis preparative (bulk) electrochemistry, see: Zizelman, P. M.; Amatore, C.; Kochi, J. K. *J. Am. Chem. Soc.* **1984**, *106*, 3771 (footnote 20); footnote 41 in ref 39; footnote 17 in ref 21a.

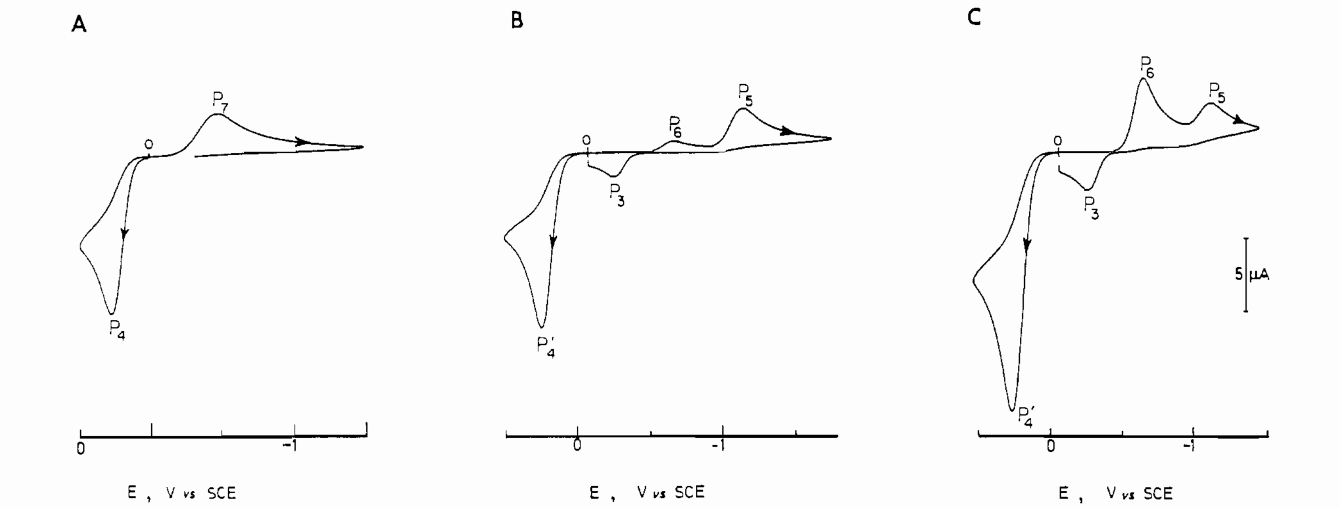

Figure 8. Initial positive scan cyclic voltammograms of 5 × 10^{-3} M $Co(CO)_4^-PPN^+$ in THF containing 0.3 M TBAP at v = 0.5 V s^{-1} in the presence of (A) 0, (B) 1, and (C) 6 equiv of added PPh_3.

Moreover this electrode process was also accompanied by a marked increase in the anodic peak current of P_4' owing to the change from the 1-electron process in eq 27 to the 2-electron process in eq 28. [Note that P_5 was only slightly affected by the presence of additional PPh_3.]

A similar CV behavior was observed with the butyl derivative $Co(CO)_3PBu_3^-$. Thus on an initial positive scan the anodic peak P_4 was observed at E_p = −0.35 V and on the return scan the cathodic peak P_5 for $Co_2(CO)_6(PBu_3)_2$ was observed at E_p = −1.66 V (Figure 7A). The addition of 1 equiv of PBu_3 yielded a cyclic voltammogram with an additional cathodic peak P_6 for $Co(CO)_3(PBu_3)_2^+$ at E_p = −1.36 V (Figure 7B). With 10 equiv of added PBu_3 only P_6 was observed on the return scan in Figure 7C. The CV behavior of $Co(CO)_3PBu_3^-$ thus differs from the phenyl analogue $Co(CO)_3PPh_3^-$ in the facility with which dimer formation (P_5) was inhibited by added PBu_3. (Compare the rapid disappearance of P_5 in Figures 6 and 7.)

The facile formation of the disubstituted cation $Co(CO)_3P_2^+$ during the initial positive scan cyclic voltammograms of $Co(CO)_3P^-$ in the presence of added phosphine (see Figure 7C) was suggestive of a rapid ligand substitution accompanying the passage of anodic current. This conclusion was indeed borne out in the cyclic voltammetry of either $Co(CO)_3PPh_3^-$ in the presence of PBu_3 or $Co(CO)_4^-$ with added PPh_3. For example, Figure 6C shows that only the substituted dimer $Co_2(CO)_6(PBu_3)_2$ was formed (P_5) on the return scan in the initial positive-scan cyclic voltammogram of $Co(CO)_3PPh_3^-$ carried out in the presence of merely 1 equiv of added PBu_3; i.e.[47]

$$Co(CO)_3PPh_3^- - e^- \xrightarrow[PBu_3]{[P_4]} \tfrac{1}{2}Co_2(CO)_6(PBu_3)_2 + PPh_3 \quad (29)$$

Likewise Figure 8A shows the initial positive-scan cyclic voltammogram of the unsubstituted $Co(CO)_4^-$ with its anodic peak P_4 at E_p = 0.28 V and, on the return scan, the cathodic peak P_7 of $Co_2(CO)_8$ at E_p = −0.49 V. However when the same cyclic voltammogram was carried out in the presence of 1 equiv of added PPh_3 the cathodic peak P_7 was absent (Figure 8B). Instead, two new cathodic waves P_5 and P_6 for the substituted carbonylcobalt dimer $Co_2(CO)_6(PPh_3)_2$ and cation $Co(CO)_3(PPh_3)_2^+$, respectively, were observed (Figure 8C); i.e.

$$Co(CO)_4^- - e^- \xrightarrow[PPh_3]{[P_4']} \tfrac{1}{2}Co_2(CO)_6(PPh_3)_2 + CO \quad (30a)$$

$$Co(CO)_4^- - 2e^- \xrightarrow[PPh_3]{[P_4']} Co(CO)_3(PPh_3)_2^+ + CO \quad (30b)$$

[Note the cathodic waves P_5 and P_6 correspond to P_1 and P_2 in Figure 4.[48]] The concomitant increase in the anodic peak current of P_4' accords with the change from a 1-electron process in eq 29 to a 2-electron process in eq 30b.

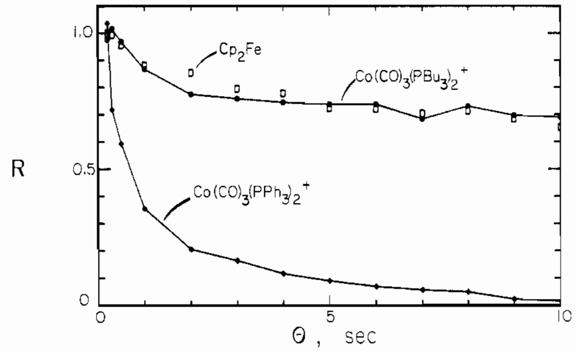

Figure 9. Variation of the normalized current ratio R with the time interval θ in the double-potential-step chronoamperometry of 5 × 10^{-3} M THF solutions of $Co(CO)_3(PBu_3)_2^+$ (●) and $Co(CO)_3(PPh_3)_2^+$ (◆) containing 0.3 M TBAP, including the external ferrocene reference (□).

E. Double potential-step chronoamperometry of the carbonylcobalt cations was carried out to establish the origin of the different CV behaviors of $Co(CO)_3(PPh_3)_2^+$ and $Co(CO)_3(PBu_3)_2^+$ in eq 25 and 26, respectively.[49] The initial pulse was set at a potential 100 mV more negative than P_1 for $Co(CO)_3P_2^+$ and following a time interval θ, the potential was stepped to a new value that was 100 mV more positive than P_3 for $Co(CO)_3P^-$ (see Figures 4 and 5). The resulting current ratio $i_a(2\theta)/i_c(\theta)$ was successively evaluated at incremental changes in θ from 0.2 to 10 s. The normalized current ratio R obtained on a basis of the 2-electron reduction of $Co(CO)_3P_2^+$ (vide supra) was plotted against θ in Figure 9. The relatively invariant line close to unity[50] for $Co(CO)_3(PBu_3)_2^+$ coincided with its 2-electron reduction to $Co(CO)_3PBu_3^-$ as described in eq 26. For $Co(CO)_3(PPh_3)_2^+$, the contrasting sharp dropoff of R from unity at θ < 1 s indicated the rapid destruction of $Co(CO)_3(PPh_3)_2^+$ by a nonfaradaic process. From the stoichiometry of the electroreduction and the dependence of i_2/i_3 on the scan rate in eq 25, we identified the side reaction as

$$Co(CO)_3PPh_3^- + Co(CO)_3(PPh_3)_2^+ \xrightarrow{<10\ s} Co_2(CO)_6(PPh_3)_2 + PPh_3 \quad (31)$$

---

[47] In addition to $Co_2(CO)_6(PBu_3)_2$ at E_p = −1.66 V, the cyclic voltammogram showed a small cathodic wave with E_p = −1.25 V that was tentatively assigned to $Co(CO)_3(PBu_3)_2^+$.

[48] The anodic wave P_3 with E_p = −0.28 V was assigned to $Co(CO)_3PPh_3^-$ in accord with Figure 4B.

[49] For a detailed description of double-potential-step chronoamperometry as applied to carbonylmetallates, see ref 21a.

[50] The slight initial dropoff at θ < 2 s was probably due to largely convectional loss of $Co(CO)_3PBu_3^-$ since parallel behavior was noted with the ferrocene external standard.

the rate of which was indicated by the facility of the ion-pair annihilation, as initially described in eq 8. By the same token, the slow rate of the analogous coupling process for the butyl analogue $Co(CO)_3(PBu_3)_2^+$ in eq 9 was responsible for the relatively invariant value of $R \sim 1$ in Figure 9. Furthermore such a marked dependence of the ion-pair coupling rates on the phosphine ligand (PPh_3 or PBu_3) readily accounted for the different preparative stoichiometries obtained in eqs 19 and 20.

Discussion

The formation of metal–metal dimers by the mutual annihilation of carbonylcobalt(I) cations and carbonylcobaltate(–I) anions is stoichiometrically represented either as a homo coupling

$$Co(CO)_3P_2^+ + Co(CO)_3P^- \rightarrow [Co(CO)_3P]_2 + P \quad (32)$$

or as a cross coupling

$$Co(CO)_3P_2^+ + Co(CO)_3P'^- \rightarrow [Co(CO)_3P]_2 + [Co(CO)_3P']_2 + Co_2(CO)_6PP' \quad (33)$$

depending on whether the same (P) or different (P,P′) phosphine ligands are employed. In order to ascertain how this distinction can be exploited, we focus on the product stoichiometry, reactivity patterns, ligand integrity, and environmental effects on the various ion-pair couplings. Before doing so however, we emphasize that the annihilation rates of carbonylcobalt ion pairs vary widely, and their reactivity patterns can thus be readily assessed,[29] without recourse to detailed kinetics analyses.

I. Accountable Facts about Ion-Pair Annihilation. Any mechanistic delineation of the ion-pair couplings associated with eqs 32 and 33 must reconcile all of the diverse experimental observations as enumerated in the following.

F-1. The homo coupling with P = PPh_3 is quantitative and rapid (eq 8), whereas the same process with P = PBu_3 is slow (eq 9).

F-2. The cross coupling with P = PPh_3 and P′ = PBu_3 is rapid, and it yields a more or less equimolar mixture of the three dicobalt carbonyls (eq 10). However the same process for the reverse combination with P = PBu_3 and P′ = PPh_3 is slow and preferentially leads to $Co_2(CO)_6P_2$ with lesser amounts of $Co_2(CO)_6PP'$ but no $Co_2(CO)_6P'_2$ (eq 11).

F-3. The homo coupling with P = PPh_3 in the presence of added PBu_3 produces only the substituted dimer $Co_2(CO)_6(PBu_3)_2$ under conditions in which neither the anion nor cation alone is subject to ligand substitution (eq 13).

F-4. The *rate* of the substitutive coupling in eq 13 is essentially unaffected by the presence of 2–10 equiv of foreign phosphine (PBu_3).[51]

F-5. Ion-pair annihilation is subject to strong retardation by polar solvents (eq 14), and it shows a pronounced negative salt effect (eq 15).

F-6. In nonpolar solvents (THF, CH_2Cl_2, etc) the carbonylcobalt cations and anions exist as contact ion pairs that are detected by their characteristic charge-transfer absorption bands (Figure 1). The formation of these contact ion pairs is inhibited by polar solvents and by added neutral salts (Figure 2).

II. Metal–Metal Dimers from Contact Ion Pairs. The diverse results described by points F-1 through F-6 cannot be explained by any single process in which the metal–metal bond for the dimer (eq 32/33) is formed by the direct replacement of a phosphine ligand (P) on the cationic $Co(CO)_3P_2^+$ by the nucleophilic anion $Co(CO)_3P^-$. Indeed the experimental observations F-3 plus F-4 demand that one or more reactive intermediates intervene between the rate-limiting activation process and the product-determining step.[52] In order to facilitate the presentation of our mechanistic analysis, we begin by noting the strong correlation of point F-5 with point F-6, in which the solvent and salt effects on the *rate* of ion-pair coupling in eq 14 and 15, respectively, are directly related to their effects on the *formation* of contact ion pairs in Figure 2a,b. Accordingly the rapid equilibria leading up to the rate-determining step can be readily summarized as in Scheme I, where the brackets enclose the contact ion pair. Values of the formation constant[31] $K > 10^4\ M^{-1}$ together with the configurational distortion of contact ion pairs in THF and CH_2Cl_2 (see IR data in Table III) point to a first-order activation process (k_1) in eq 35.

Scheme I

$$Co(CO)_3P_2^+ + Co(CO)_3P^- \overset{K}{\rightleftharpoons} [Co(CO)_3P_2^+][Co(CO)_3P^-] \quad (34)$$

$$[Co(CO)_3P_2^+][Co(CO)_3P^-] \xrightarrow{k_1} Co_2(CO)_6P_2 + P \quad (35)$$

III. Ion-Pair Annihilation by Electron Transfer. The extensive scrambling of the ligands during ion-pair annihilation as established by points F-2 and F-3 further indicates that eq 35 in Scheme I must proceed via labile intermediates.[53] Accordingly we initially elaborated the rate-limiting activation as an electron-transfer process.[54] On this basis the sequence of reactions leading to the metal-metal dimers evolve spontaneously from a pair of 19- and 17-electron carbonylcobalt radicals, as presented in Scheme II for the homo-coupling process.

Scheme II

$$[Co(CO)_3P_2^+][Co(CO)_3P^-] \xrightarrow{k_1} Co(CO)_3P_2^\bullet + Co(CO)_3P^\bullet \quad (36)$$

$$Co(CO)_3P_2^\bullet \rightleftharpoons Co(CO)_3P^\bullet + P \quad (37)$$

$$2Co(CO)_3P^\bullet \rightarrow Co_2(CO)_6P_2 \quad (38)$$

Previous studies have indeed established both the substitutional lability and the rapid dimerization of carbonylcobalt and related radicals.[55-57] According to Scheme II, the extensive scrambling of the phosphine ligands P and P′ during cross coupling (eq 10–12) derives from the facile and reversible interconversion of radical pairs; i.e.

$$\underset{(17e^-)}{Co(CO)_3P'^\bullet} + P \rightleftharpoons \underset{(19e^-)}{Co(CO)_3P'P^\bullet} \rightleftharpoons \underset{(17e^-)}{Co(CO)_3P^\bullet} + P' \quad (39)$$

In order to ascertain the viability of this mechanistic formulation, let us now turn to the preparative and transient electrochemical experiments that directly bear on the behavior of 19- and 17-electron carbonylcobalt radicals formed under the conditions of ion-pair annihilation. Thus the high yields of homo-coupled dimers that are isolated from both the electroreduction of the cationic $Co(CO)_3P_2^+$ (Table IV) as well as the electrooxidation of the anionic $Co(CO)_3P^-$ (Table V) confirm the rapid coupling of the carbonylcobalt radicals, as in eq 38. Relevant to the facile ligand substitution of carbonylcobalt radicals (eq 39) is the formation of the PPh_3-substituted cobalt dimer when the oxidation of carbonylcobaltate is carried out in the presence of added triphenylphosphine in eq 22.

IV. Dynamic Behavior of 19- and 17-Electron Carbonylcobalt Radicals. The series of transient electrochemical studies with cyclic voltammetry establish the kinetic behavior of (A) the 19-electron radical from the reduction of $Co(CO)_3P_2^+$ and (B) the 17-electron

---

(51) However at high concentration of PBu_3 (<30 equiv) the rate of the substitutive ion-pair coupling is retarded. Compare with footnote 44.

(52) Lewis, E. S.; Boozer, C. E. In Investigation of Rates and Mechanisms of Reactions. Technique *of Organic Chemistry*; Weissberger, A., Ed.; Wiley: New York, 1963; Vol. VIII.

(53) See the accounting of point F-3 plus point F-4 with ref 52.

(54) Other pathways, such as ligand substitution of either $Co(CO)_3P_2^+$ or $Co(CO)_3P^-$ that precedes ion-pair coupling, are ruled out by the substantially inert character of both the carbonylcobalt cation and anion.

(55) (a) Mugnier, Y.; Reeb, P.; Moise, C.; Laviron, E. *J. Organomet. Chem.* **1983**, *254*, 111. (b) Reeb, P.; Mugnier, Y.; Moise, C.; Laviron, E. *J. Organomet. Chem.* **1984**, *273*, 247.

(56) Wegman, R. W.; Brown, T. L. *Inorg. Chem.* **1983**, *22*, 183. Compare also: Wegman, R. W.; Olsen, R. J.; Gard, D. R.; Faulkner, L. R.; Brown, T. L. *J. Am. Chem. Soc.* **1981**, *103*, 6089. Walker, H. W.; Herrick, R. S.; Olsen, R. J.; Brown, T. L. *Inorg. Chem.* **1984**, *23*, 3748. Absi-Halabi, M.; Brown, T. L. *J. Am. Chem. Soc.* **1977**, *99*, 2982. For steric effect of phosphines, see: Tolman, C. A. *Chem. Rev.* **1977**, *77*, 313.

(57) Cf. also ref 20.

radical from the oxidation of $Co(CO)_3P^-$ that are critical to the redox process (eq 36) as follows.[58]

A. The 19-electron radicals $Co(CO)_3P_2^•$ are generated (P_1) in the initial negative-scan cyclic voltammetry of the cationic $Co(CO)_3P_2^+$. The results in Figures 4 and 5 together with the double-potential-step chronoamperometry in Figure 9 delineate the transient behavior during electroreduction as an ECE process as in Scheme III.[59,60]

Scheme III

$$Co(CO)_3P_2^+ \xrightarrow{e^-} Co(CO)_3P_2^• \qquad (40)$$

$$Co(CO)_3P_2^• \rightleftharpoons Co(CO)_3P^• + P \qquad (41)$$

$$Co(CO)_3P^• \xrightarrow{e^-} Co(CO)_3P^- \qquad (42)$$

The extent to which the cobalt dimer is observed by its cathodic wave P_2 during cyclic voltammetry derives in a subsequent (nonfaradaic) sacrificial destruction of $Co(CO)_3P^-$ by its cationic precursor;[61] i.e.

$$Co(CO)_3P^- + Co(CO)_3P_2^+ \rightarrow Co_2(CO)_6P_2 + P \qquad (43)$$

The scan rate dependence of the cyclic voltammograms (Figure 4c and 5c) shows that dimer formation by eq 43 is rapid for P = PPh_3 (see eq 31) but slow for P = PBu_3. Indeed this CV distinction between $Co(CO)_3(PPh_3)_2^+$ and $Co(CO)_3(PBu_3)_2^+$ mirrors the results obtained in ion-pair annihilation (see Section I.E). As such, the rate of ion-pair annihilation will parallel the driving force for electron transfer in eq 36 (Scheme II) as given by the relationship

$$\Delta G_{et} \simeq -\mathcal{F}(E_c - E_a) \qquad (44)$$

where E_c and E_a are peak potentials in Table VI for the CV waves P_1 and P_3 (Figures 4 and 5).[62] Evaluated in this way, the driving force for electron transfer of the PPh_3-substituted ion pair is substantially (~13 kcal mol^{-1}) greater than that for the PBu_3-substituted ion pair. This conclusion thus accounts for the reactivity pattern established by point F-1 for homo coupling, and the same reasoning leads to point F-2 for cross coupling.

B. The 17-electron radicals $Co(CO)_3P^•$ are generated (P_4) in the initial positive-scan cyclic voltammetry of the anionic $Co(CO)_3P^-$. The results in Figures 6a and 7a point to the transient behavior during electrooxidation as an $\bar{E}C$ process as in Scheme IV.[63,64]

Scheme IV

$$Co(CO)_3P^- \xrightarrow{-e^-} Co(CO)_3P^• \qquad (45)$$

$$2Co(CO)_3P^• \rightarrow Co_2(CO)_6P_2 \qquad (46)$$

More relevant to the lability of 17-electron radicals is the effect of added phosphine, as shown in Figures 6b and 7b; i.e.[65,66]

$$Co(CO)_3P^• + P \rightleftharpoons Co(CO)_3P_2^• \qquad (47)$$

$$Co(CO)_3P_2^• \xrightarrow{-e^-} Co(CO)_3P_2^+ \qquad (48)$$

In the same vein, the addition of a foreign phosphine P′, in eq 47 leads to the substituted cobalt dimer $Co_2(CO)_6P_2'$ and cation $Co(CO)_3(P_2')^+$ (Figures 6c and 8c), in accord with the formulation in eq 39. Most importantly, the observation of these processes on the CV time scale of milliseconds confirms the rapidity with which ligand substitution occurs on the 17-electron radicals $Co(CO)_3P^•$.[55-57] Therefore we conclude that the extensive scrambling of phosphine ligands as delineated in points F-2 and F-3 provides the most compelling experimental support for carbonylcobalt radicals as reactive intermediates. As such, the electron-transfer mechanism in Schemes I and II taken together reconcile the diverse experimental facets of ion-pair annihilation, such as all those included in points F-1 through F-6. However, before this formulation is embraced too strongly as a general mechanism, cognizance must be taken of alternative pathways.

V. Comments on the Coupling of Disproportionation Ion Pairs. The annihilation of the disproportionation ion pair $[Co(CO)_3(PBu_3)_2^+][Co(CO)_4^-]$ obtained from dicobalt octacarbonyl and tri-*n*-butylphosphine proceeds much more slowly (eq 12) than that for the analogous PPh_3-substituted ion pair.

$$[Co(CO)_3(PPh_3)_2^+][Co(CO)_4^-] \rightarrow [Co(CO)_3PPh_3]_2 + CO \qquad (49)$$

For example, the conversion to $Co_2(CO)_6(PBu_3)_2$ proceeds to only 5% within a 60-h period, whereas the formation of $Co_2(CO)_6(PPh_3)_2$ in eq 49 is complete within 8 h under the same reaction conditions. According to Scheme II, such a large difference in annihilation rates between these ion pairs arises from the sizable difference of ~15 kcal mol^{-1} in the driving force ΔG_{et} for electron transfer (see Table VI and eq 44). However the recent study of $[Co(CO)_3(PPh_3)_2^+][Co(CO)_4^-]$ led to an entirely different mechanistic conclusion[17] that is summarized in Scheme V.

Scheme V

$$Co(CO)_3(PPh_3)_2^+ \xrightarrow{k_1} Co(CO)_2(PPh_3)_2^+ + CO \qquad (50)$$

$$Co(CO)_2(PPh_3)_2^+ + Co(CO)_4^- \xrightarrow{\text{fast}} (OC)_4CoCo(CO)_2(PPh_3)_2 \qquad (51)$$

$$(OC)_4CoCo(CO)_2(PPh_3)_2 \xrightarrow[\upsilon]{\text{fast}} [Co(CO)_3PPh_3]_2 \qquad (52)$$

The rate-limiting CO dissociation in eq 50 was based largely on an observed first-order rate constant $k_1 = 2.1 \times 10^{-4}\ s^{-1}$ for ion-pair annihilation that was essentially the same as the first-order rate constant k_{ex} for isotopic CO exchange of $Co(CO)_3(PPh_3)_2^+BPh_4^-$, together with the reduced value of $k_1 = 1.1 \times 10^{-4}\ s^{-1}$ obtained in the presence of 1 atm of added CO.[17] Otherwise, most of the other experimental observations in this system (eq 49) paralleled the results of our study, viz., retardation by polar solvents, negative salt effect, and the neutrality of added PPh_3 on the annihilation rate. Indeed the observation of first-order kinetics[17] is also a strong confirmation of the importance of contact ion pairs as presented in Scheme I.[67] While our studies do not bear directly on the validity of Scheme V for the disproportionation ion pair $[Co(CO)_3(PPh_3)_2^+][Co(CO)_4^-]$, there is compelling evidence that rules out such a dissociative formulation as a general mechanism. Thus a rate-limiting loss of ligand (either CO or P) cannot explain the ion-pair couplings in both eq 8 and 10 that occur rapidly upon mixing (<5 min) of the otherwise substitu-

---

(58) For a related CV study of 19-e and 17-e carbonylmanganese radicals, see: (a) Amatore, C.; Kuchynka, D. J.; Kochi, J. K. *J. Electroanal. Chem. Interfacial Electrochem.* **1988**, *241*, 181. (b) Kuchynka, D. J.; Kochi, J. K. *J. Am. Chem. Soc.* Submitted for publication. (c) Reference 21a.

(59) Although it is possible that the reduction of $Co(CO)_3P_2^+$ occurs by dissociative electron attachment (i.e. eq 40 and 41 in one step) there is independent evidence for the existence of 19-e carbonylmetal radicals, however transitory.[58b]

(60) In this *cathodic* process, the 17-e radical is rapidly reduced (eq 42), and its lifetime is too short for significant competition of second-order dimerization. See footnote 34 in ref. 21a.

(61) The different stoichiometries obtained in the preparative electrooxidation of $Co(CO)_3(PPh_3)_2^+$ and $Co(CO)_3(PBu_3)_2^+$ in eq 19 and 20 also relate to the CV behaviors in Figures 4B and 5A, respectively. See also the discussion in footnote 46.

(62) Equation 44 is based on the use of irreversible CV peak potentials in parallel behavior to the reversible electrode potentials. See, e.g.: (a) Klingler, R. J.; Kochi, J. K. *J. Am. Chem. Soc.* **1980**, *102*, 4790; *J. Phys. Chem.* **1981**, *85*, 1731. (b) Miller, L. L.; Nordblom, G. D.; Mayeda, E. A. *J. Org. Chem.* **1972**, *37*, 917. (c) Bard, A. J.; Faulkner, L. R. *Electroanalytical Methods*; Wiley: New York, 1980.

(63) (a) In this *anodic* process, the dimerization of 17-electron radicals dominates—in contrast to the cathodic situation in Scheme III (see footnote 60). (b) For a detailed mechanistic description of the EC process, see ref 58b and 64.

(64) Olmstead, M. L.; Hamilton, R. G.; Nicholson, R. S. *Anal. Chem.* **1969**, *41*, 260.

(65) It is important to note that 19-electron radicals such as $Co(CO)_3P_2^•$ are easier to oxidize (i.e., at less positive potentials) than their 17-electron counterparts $Co(CO)_3P^•$ (see ref 58b and 66).

(66) Compare: Kuchynka, D. J.; Kochi, J. K. *Inorg. Chem.* **1988**, *27*, 2574.

(67) The spectroscopic study of the contact ion pair $[Co(CO)_3(PPh_3)_2^+][Co(CO)_4^-]$ in eq 49 is not so apparent from its CT spectrum. See footnote 38.

tion-inert $Co(CO)_3(PPh_3)_2^+$ cation.[54] In fact, the electron-transfer formulation in Scheme II will readily accommodate all of the experimental facts extant for the annihilation of $[Co(CO)_3(PPh_3)_2^+][Co(CO)_4^-]$—with the one exception bearing on the coincidence of k_1 and k_{ex}.[68] Importantly, the monosubstituted $Co_2(CO)_7PPh_3$ and not the symmetrical $Co_2(CO)_6(PPh_3)_2$ in eq 49 was the principal dimeric product observed under an atmosphere of CO;[17] i.e.

$$[Co(CO)_3(PPh_3)_2^+][Co(CO)_4^-] \xrightarrow{CO} (OC)_4CoCo(CO)_3PPh_3 + PPh_3 \quad (53)$$

The preferential formation of $Co_2(CO)_7PPh_3$ in eq 53 naturally follows from Scheme II since the preponderance of the 19-electron radicals formed under these conditions is expected to be $Co(CO)_4P^\bullet$; i.e.

$$Co(CO)_3P^\bullet + CO \rightleftharpoons Co(CO)_4P^\bullet \rightleftharpoons P + Co(CO)_4^\bullet \quad (54)$$

in a manner entirely analogous to the series of rapid equilibria established in eq 39.[69] It is less obvious how the dissociative mechanism in Scheme V can account for $Co_2(CO)_7PPh_3$ since a CO-induced replacement of one PPh_3 ligand in $Co(CO)_3(PPh_3)_2^+$ to afford $Co(CO)_4PPh_3^+$ is without precedent.[72]

Experimental Section

Materials. Triphenylphosphine (Aldrich) and tri-*p*-tolylphosphine (M and T) were recrystallized from ethanol prior to use. Tri-*n*-butylphosphine (M and T) was distilled and stored in a Schlenk flask under an argon atmosphere. Dicobalt octacarbonyl (Pressure Chemical) was used without further purification. $Co(CO)_3(PBu_3)_2^+ClO_4^-$ was prepared from $Co(ClO_4)_2\cdot 6H_2O$ and 6 equiv of tri-*n*-butylphosphine in isopropyl alcohol under a CO atmosphere at room temperature for 24 h.[25] The precipitate was collected and recrystallized from a mixture of methylene chloride and ethyl ether. All other cations, $Co(CO)_3(PPh_3)_2^+BF_4^-(PF_6^-)$, and $Co(CO)_3[P(p\text{-tol})_3]_2^+PF_6^-$ were prepared from dicobalt octacarbonyl and 2 equiv of the appropriate phosphine in methylene chloride or dioxane at room temperature for 30 min.[9] $Co(CO)_3P_2^+Co(CO)_4^-$ was oxidatively metathesized by using $Cp_2Fe^+BF_4^-(PF_6^-)$.[24b] For example, $Co(CO)_3P_2^+Co(CO)_4^-$ with 2 equiv of the ferrocenium salt and 2 equiv of the corresponding phosphine was stirred in methylene chloride until the purple color of the ferrocenium cation was discharged. The desired salt was precipitated by addition of hexane. These salts were also prepared directly from $Co_2(CO)_8$, 2 equiv of ferrocenium salt and 4 equiv of the suitable phosphine in methylene chloride.[24a] Purification was effected by recrystallization from a mixture of dichloromethane and hexane. The cobaltcarbonyl dimers $Co_2(CO)_6(PPh_3)_2$ and $Co_2(CO)_6(PBu_3)_2$ were prepared as described in the literature.[11] Thus, 3 equiv of the appropriate phosphine was slowly added to a solution of octacarbonyl dicobalt in benzene. The reaction mixture was refluxed for 2–6 h. The PPh_3 and $P(p\text{-tol})_3$ derivatives precipitated during the reaction and they were collected, washed with hexane, and used without further purification. The other dimers were isolated by evaporation of solvent and recrystallized from either hexane or benzene.

$Co(CO)_4^-Na^+$ was prepared according to the literature procedure[28] by treating $Co_2(CO)_8$ with powdered NaOH in THF. After 2 h, the pale yellow solution was separated from the purple NaOH residue and the solvent was evaporated in vacuo. The sodium salt was metathesized with PPN^+Cl^- in dichloromethane.[27] NaCl was removed by filtration, and the solvent was evaporated. The colorless $Co(CO)_4^-PPN^+$ was recrystallized from a mixture of dichloromethane and ethyl ether. Air-sensitive anions such as $Co(CO)_3PPh_3^-$ [26] and $Co(CO)_3PBu_3^-$ [17] were prepared from $Co_2(CO)_6(PPh_3)_2$ and $Co_2(CO)_6(PBu_3)_2$, respectively, by sodium amalgam reduction. Typically, the dimer $Co_2(CO)_6P_2$ in THF was treated with freshly made sodium amalgam from 0.11 g of sodium and 1 mL of mercury. After the reaction was stirred for 1 h under an argon atmosphere, the excess mercury amalgam was removed and the mixture was filtered through Celite under an argon atmosphere. The complete conversion of the dimer to the anion was monitored by IR analysis. The sodium salt was metathesized with PPN^+Cl^- in THF as follows. $Co(CO)_3P^-Na^+$ and 1 equiv of PPN^+Cl^- was stirred in THF as a slurry for 1 h. After removal of the mixture consisting of NaCl and unreacted PPN^+Cl^-, the solution was concentrated in vacuo. Purification was effected by recrystallization from a mixture of THF and ethyl ether.

Tetrahydrofuran was distilled from sodiobenzophenone and stored in a Schlenk flask under an argon atmosphere. Acetonitrile was initially stirred over potassium permanganate for 12 h, and the mixture was then refluxed for an additional hour. After filtration, the colorless liquid was treated with diethylenetriamine and filtered again. It was finally fractionated from phosphorus pentoxide under an argon atmosphere. Tetra-*n*-butylammonium perchlorate (TBAP; G. F. Smith Chemical) was recrystallized from ethyl acetate and dried in vacuo.

Instrumentation and Electrochemical Methods. IR spectra were obtained with NaCl cells (0.1 mm) by using a Nicolet 10 DX FT spectrometer with 4 cm^{-1} resolution. ^{31}P NMR spectra were recorded on a JEOL FX90Q FT spectrometer. UV/vis spectra were obtained on a Hewlett-Packard 8450A diode array spectrophotometer. Reflectance UV/vis spectra were recorded on a Perkin-Elmer 330 spectrometer equipped with a Hitachi Model H210-2101 integrating sphere accessory. Cyclic voltammetry was performed on an *iR*-compensated potentiostat[73] driven by a Princeton Applied Research Model 175 universal programmer. The high-impedence voltage follower was mounted external to the potentiostat to minimize noise pickup. CV curves were either displayed on a Tektronix Model 5115 storage oscilloscope or recorded on a Houston Series 2000 X-Y recorder. The aging of the solutions was generally not a problem, and the potential/current profiles could be reproduced throughout the experiment. The platinum electrode was periodically polished with a fine emery cloth. The CV cell was of airtight design and was equipped with high-vacuum Teflon valves and Vitron O-ring seals to allow an inert atmosphere to be maintained without contamination by grease. The adjustable working electrode consisted of a platinum disk embedded in a glass seal to allow periodic polishing without changing the surface area (~1 mm^2) significantly. The counter electrode consisting of a platinum gauze was separated from the working electrode by less than 2 mm and connected to the reference electrode via a 0.02 μF capacitor to aid in the compensation of the *iR* drop.

Procedures for Ion-Pair Coupling. $Co(CO)_3PPh_3^-$ + $Co(CO)_3(PPh_3)_2^+$. The addition of 5 mL of a 1 × 10^{-2} M $Co(CO)_3PPh_3^-Na^+$ solution in THF to 5 mL of a 1 × 10^{-2} M $Co(CO)_3(PPh_3)_2^+PF_6^-$ solution in THF resulted in an instantaneous precipitation of a red solid. The first IR spectrum recorded within 5 min showed no carbonyl band other than that of $Co_2(CO)_6(PPh_3)_2$ in trace amounts. The red solid was identified as $Co_2(CO)_6(PPh_3)_2$ from the IR spectrum in a KBr pellet. Yield: 36.5 mg (90%). Triphenylphosphine was extracted from the residue with hexane. Yield: 21.0 mg. The ion-pair coupling was also carried out in THF containing 0.3 M TBAP or in acetonitrile. The results were similar, the reactions being completed within 5 min to afford $Co_2(CO)_6(PPh_3)_2$ in addition to PPh_3. However, the coupling of $Co(CO)_3PPh_3^-$ and $Co(CO)_3(PPh_3)_2^+$ in the presence of 30 equiv of PBu_3 required 30 min for both starting materials to disappear. The solution became red and there was no discernible precipitation from solution. The product was identified as $Co_2(CO)_6(PBu_3)_2$ from the IR band at ν_{CO} = 1944 cm^{-1}. In order to check for ligand exchange of $Co(CO)_3P_2^+$, a 20 mM solution of $Co(CO)_3[P(p\text{-tol})_3]_2^+PF_6^-$ in THF was treated with 1 equiv of triphenylphosphine in a NMR tube. The ^{31}P NMR spectrum was recorded at 30 min intervals. After 2 h, no broadening of the resonance at δ 52.7 ppm was observed nor was a new peak due to free tritolylphosphine observed. Owing to the low solubility of $Co(CO)_3(PPh_3)_2^+PF_6^-$ in THF, the reverse combination was not examined. Furthermore $Co(CO)_3[P(p\text{-tol})_3]_2^+$ was inert to ligand exchange with 5 equiv of added PPh_3. A similar experiment was performed with $Co(CO)_3[P(p\text{-tol})_3]_2^+PF_6^-$ and 5 equiv of PBu_3. No detectable change in the ^{31}P NMR spectrum was detected after 2 h.

$Co(CO)_3PBu_3^-$ + $Co(CO)_3(PBu_3)_2^+$. A 5 mL solution of 1 × 10^{-2} M $Co(CO)_3(PBu_3)^-Na^+$ in THF was added to a 1 × 10^{-2} M solution of

---

(68) Except for experimental values of k_1 and k_{ex} that are fortuitously degenerate, the relationship $k_1 = k_{ex}$ does not follow easily from Scheme II. Note that the straight application of Scheme V to the ion pairs examined in this study would lead to the tris(phosphine)-substituted dimers $Co_2(CO)_5P_3$.

(69) Furthermore, the buildup of the 19-electron radicals in the presence of *excess* ligand (CO) will lead to rate retardation[51] by increasing the rate of the back reaction for eq 36.[70,71] For evidence of reversibility in electron-transfer processes such as eq 36, see: ref 58b and 66.

(70) Since this is a secondary effect, rate-retardation is much less important at low concentrations of added ligand such as in point F-4.

(71) Compare: (a) Payne, M. W.; Leussing, D. L.; Shore, S. G. *J. Am. Chem. Soc.* **1987**, *109*, 617. (b) Ungvary, F.; Wojcicki, A. *J. Am. Chem. Soc.* **1987**, *109*, 6848.

(72) (a) For example, compare the negligible effect of CO in the preparative procedures described by Rigo et al. in ref 25 and by: Imyanitov, N. S.; Volkov, V. A. *J. Gen. Chem. USSR* **1974**, *44*, 2741. (b) It is possible that the replacement PPh_3 by CO occurs subsequent to the rate-limiting step (e.g., in eq 52).

(73) (a) Garreau, D.; Saveant, J. M. *J. Electroanal. Chem. Interfacial Electrochem.* **1972**, *35*, 309. (b) Garreau, D.; Saveant, J. M. *J. Electroanal. Chem. Interfacial Electrochem.* **1974**, *50*, 22.

$Co(CO)_3(PBu_3)_2{}^+ClO_4{}^-$ in 5 mL of THF. The starting materials completely disappeared after 30 min, as monitored by IR spectroscopy. $Co_2(CO)_6(PBu_3)_2$ was the only cobaltcarbonyl product observed. The solution was concentrated, and $Co_2(CO)_6(PBu_3)_2$ was extracted from the residue with hexane. Yield: 32 mg (93%). When the same coupling was performed in THF containing 0.3 M TBAP, the reaction proceeded slowly. After 10 h, $Co(CO)_3PBu_3{}^-$ slowly disappeared. However the carbonyl absorption due to $Co(CO)_3(PBu_3)_2{}^+$ was unchanged. Instead, the absorbance at 1887 cm^{-1} increased gradually, and $Co_2(CO)_6(PBu_3)_2$ was observed in trace amounts.

$Co(CO)_3PBu_3{}^-$ + $Co(CO)_3(PPh_3)_2{}^+$. An 8 mL solution of 1×10^{-2} M $Co(CO)_3PBu_3{}^-$ in THF was treated with 8 mL of 1×10^{-2} M $Co(CO)_3(PPh_3)_2{}^+$ in THF. Immediate precipitation occurred upon mixing. The first IR spectrum recorded within 5 min showed no starting material—only a strong band at 1946 cm^{-1}. Four components were detected by TLC on silica gel (hexane/THF = 4/1, v/v) with R_f values at 0.58, 0.51, 0.41, and 0.0. By comparison with an authentic sample, the spot with R_f = 0.51 coincided with that of triphenylphosphine. Filtration of the precipitate yielded 23.4 mg of $Co_2(CO)_6(PPh_3)_2$ (R_f = 0.0). The filtrate was concentrated and eluted on a silica gel column in the dark (hexane/THF = 9/1, v/v) to yield the following compounds: $Co_2(CO)_6(PBu_3)_2$, 15.2 mg, R_f = 0.58; $Co_2(CO)_6(PBu_3)(PPh_3)$, 17.3 mg, R_f = 0.41. Anal. Calcd for $C_{36}H_{42}Co_2O_6P_2$: C, 57.60; H, 5.65. Found: C, 58.20; H, 6.13. The mixed dimer $Co_2(CO)_6(PBu_3)(PPh_3)$ was also obtained from the photolysis of a mixture of $Co_2(CO)_6(PPh_3)_2$ and $Co_2(CO)_6(PBu_3)_2$ in THF at low conversions.[20]

$Co(CO)_3PPh_3{}^-$ + $Co(CO)_3(PBu_3)_2{}^+$. A reaction with 5 mM mixture of each ion in 16 mL of THF was completed after 30 min. The solution became red, but no precipitate was observed. The IR spectrum after 30 min showed a strong but broad absorption band at 1945 cm^{-1}. On TLC analysis (hexane/THF = 4/1, v/v), three spots were detected at R_f = 0.58, 0.51, and 0.41. No residual spot was observed at the origin. By comparison with an authentic sample, the components with R_f = 0.58, 0.51, and 0.41 coincided with $Co_2(CO)_6(PBu_3)_2$, PPh_3 and $Co_2(CO)_6(PPh_3)(PBu_3)$ respectively. The products were separated on a silica gel column by eluting with a mixture of hexane and THF [9/1 (v/v)] in the dark. Yield: $Co_2(CO)_6(PBu_3)_2$, 29.7 mg (54%); $Co_2(CO)_6(PBu_3)(PPh_3)$, 15.8 mg (26%). ν_{CO} = 1970 (vw), 1950 cm^{-1} (vs) in THF. This ion-pair coupling was also carried out in NMR tube. After 1 h of accumulation, the ^{31}P NMR spectrum showed the presence of free PPh_3 at −5.7 ppm together with free $P(n\text{-}Bu)_3$ at −32.1 ppm (relative to 85% phosphoric acid). The strong resonance at δ 52.3 ppm and the weak resonance at δ 66.9 ppm were assigned to $Co_2(CO)_6(PBu_3)_2$ and $Co_2(CO)_6(PBu_3)(PPh_3)$. The control reaction of $Co_2(CO)_6(PPh_3)(PBu_3)$ with 1 equiv of PBu_3 was very slow, and only after 2 h was a trace of $Co_2(CO)_6(PBu_3)_2$ detected by TLC analysis. The coupling of $Co(CO)_3PPh_3{}^-$ and $Co(CO)_3(PBu_3)_2{}^+$ in acetonitrile did not show any appreciable conversion even after 10 h. The coupling of 5 mL of 1×10^{-2} M solution of $Co(CO)_3PPh_3{}^-Na^+$ in THF with 5 mL of 1×10^{-2} M solution of $Co(CO)_3(PBu_3)_2{}^+ClO_4{}^-$ in THF containing 0.6 M TBAP proceeded very slowly. After 10 h, the 5% decrease of the absorptions due to the cation and anion was observed and small peak due to dimeric cobalt was detected. The nature of product having a broad absorption at 1945 cm^{-1} was not determined.

$Co(CO)_3(PPh_3)_2{}^+$ + $Co(CO)_3PPh_3{}^-$ and Added PBu_3. To 5 mL of 10^{-2} M $Co(CO)_3(PPh_3)_2{}^+$ in THF containing various amounts of PBu_3 was added 5 mL of 10^{-2} M $Co(CO)_3PPh_3{}^-$ in THF. The reaction mixture turned red, and the $Co(CO)_3(PPh_3)_2{}^+$ salt dissolved completely. The course of reaction was followed by IR analysis. In those systems containing 2–15 equiv of added PBu_3 the reactions were all complete within <5 min. However the presence of 20 equiv of added PBu_3 led to slight retardation. Thus the first IR spectrum taken after 5 min showed only small amounts (<10%) of unreacted cation and anion. After 15 min, both starting materials were completely consumed. On the other hand, dramatic changes occurred in the product distributions. In contrast to the ion-pair coupling carried out with no added PBu_3, $Co_2(CO)_6(PPh_3)_2$ was not observed. Instead, the substituted dimer $Co_2(CO)_6(PBu_3)_2$ was the major product, and the mixed $Co_2(CO)_6(PPh_3)(PBu_3)$ was also detected as minor product on TLC analysis when 2, 4, or 6 equiv of PBu_3 were present. R_f for $Co_2(CO)_6(PBu_3)_2$ was 0.58 and for $Co_2(CO)_6(PPh_3)(PBu_3)$ was 0.41 with 4/1 vol/vol hexane and THF on silica gel. Yield (%) of $Co_2(CO)_6(PBu_3)_2$ and $Co_2(CO)_6(PPh_3)(PBu_3)$ and amount added PBu_3 (equiv): 90, 10, 2; 80, 6, 4; 80, 1, 6; 80, 0, 10; 70, 0, 15; 80, 0, 20.

Spectral Examination of Carbonylcobalt Salts. The IR spectra of $[Co(CO)_3(PPh_3)_2{}^+][Co(CO)_4{}^-]$ and $[Co(CO)_3(PBu_3)_2{}^+][Co(CO)_4{}^-]$ were measured as 5 mM in solutions in various solvents. The solid-state IR spectra of the carbonylcobalt salts either as KBr pellets or as Nujol mulls were also recorded at room temperature.

The UV-vis spectra of these salts were measured at various temperatures in order to assess the extent of the interference from thermal processes. All samples were prepared and measured in the dark. For $[Co(CO)_3(PPh_3)_2][Co(CO)_4]$, the solution of the salt in either acetonitrile or methylene chloride was prepared at room temperature, and spectra were measured quickly. However for the spectral measurements in THF solutions, the samples were prepared at −30 °C at which any thermal process was negligible. The UV spectra of the separate components, $Co(CO)_3(PPh_3)_2{}^+PF_6{}^-$ and $Co(CO)_4{}^-PPN^+$ were also measured for comparison. The UV spectrum of $[Co(CO)_3(PBu_3)_2][Co(CO)_4]$ was measured at room temperature in acetonitrile, CH_2Cl_2 and THF, at −40 °C in chlorobenzene and *p*-chlorotoluene, and at −78 °C in diethyl ether. In diethyl ether, the salt was partially insoluble. The thermal product was identified as $Co_2(CO)_6(PBu_3)_2$ with λ_{max} at 369 nm in ethyl ether and 289 nm (in chlorobenzene), both bands tailing out to >500 nm. The UV-vis spectra of the mixture of $Co(CO)_3PPh_3{}^-PPN^+$ and $Co(CO)_3(PBu_3)_2{}^+ClO_4{}^-$ and that of $Co(CO)_3PBu_3{}^-PPN^+$ and $Co(CO)_3(PBu_3)_2{}^+ClO_4{}^-$ were measured in THF at −78 °C and in acetonitrile at −25 °C.

Preparative Electrolysis of Carbonylcobalt Salts. Typically, the bulk electrochemical experiments were carried out potentiostatically at 25 °C in 30 mL of THF solution containing 0.3 mmol of $Co(CO)_3P_2{}^+$ or $Co(CO)_3P^-$ salt and 0.3 M TBAP (see Tables IV and V). The electrochemical cell was of airless design and allowed an extra electrode to be accommodated to monitor conveniently the solution by cyclic voltammetry during the electrolysis.[74] The constant electrode potential was maintained with a PAR 173 potentiostat/galvanostat equipped with a PAR 179 digital coulometer, both of which provided a feedback compensation for ohmic drop between the working and reference electrodes. The voltage-follower amplifier (PAR Model 178) was mounted external to the potentiostat with a minimum length of high impedence connection to the reference electrode. A 0.1-μF capacitor was connected between the voltage-follower amplifier lead and the counter electrode to ensure low noise pickup.

Double-Potential-Step Chronoamperometry of $Co(CO)_3P_2{}^+$. Double-potential-step chronoamperometry was carried out in the same electrochemical cell (vide supra). The PAR 175 programmer was set up to perform a cathodic potential step at V_1, 100 mV past the cathodic wave of $Co(CO)_3P_2{}^+$. After the interval θ, the potential was jumped to V_2, 100 mV more positive than that of the anodic wave of $Co(CO)_3P^-$ for the same time θ. For $Co(CO)_3(PBu_3)_2{}^+$, V_1 was −1.46 V and V_2 was −0.25 V. The duration of the pulse θ was typically varied at 0.2, 0.3, 0.5, 1, 2, 3, 4, 5, 6, 7, 8, 9, and 10 s. The ratio r of cathodic current to anodic current at every θ was evaluated as $|i_a(2\theta)/i_c(\theta)|$. The current ratio r was normalized with the theoretical value, 0.1465, based on a 2-electron process for the reduction of $Co(CO)_3P_2{}^+$ and a 1-electron process for the oxidation of $Co(CO)_3P^-$[75] to provide $R = r(0.1465)^{-1}$ as follows. For $Co(CO)_3(PPh_3)_2{}^+$ [θ (s), R]: 0.2, 1.037; 0.3, 0.717; 0.5, 0.594; 1.0, 0.355; 2.0, 0.205; 4.0, 0.116; 6.0, 0.068; 8.0, 0.048; 10.0, 0.014. For $Co(CO)_3(PBu_3)_2{}^+$ [θ (s), R]: 0.2, 0.976; 0.3, 1.017; 0.5, 0.969; 1.0, 0.867; 2.0, 0.774; 4.0, 0.744; 6.0, 0.737; 8.0, 0.730; 10.0, 0.689. For calibration, the experimental current ratio r for ferrocene was normalized to R by using the factor 0.293 (theoretical value for a 1-electron process for both oxidation and reduction). The normalized current ratio R for ferrocene was plotted vs θ, and matched the result for $Co(CO)_3(PBu_3)_2{}^+$ as shown in Figure 9.

Acknowledgment. We thank D. J. Kuchynka and T. M. Bockman for helpful discussions and the National Science Foundation and Robert A. Welch Foundation for financial support.

Registry No. $Co(CO)_3(PPh_3)_2{}^+PF_6{}^-$, 17787-17-6; $Co(CO)_3[P(p\text{-}tol)_3]_2{}^+PF_6{}^-$, 118400-43-4; $Co(CO)_3(PBu_3)_2{}^+ClO_4{}^-$, 38435-80-2; $Co(CO)_4{}^-PPN^+$, 53433-12-8; $Na^+Co(CO)_3PPh_3{}^-$, 33570-17-1; $Co(CO)_3PPh_3{}^-PPN^+$, 67517-68-4; $Na^+Co(CO)_3PBu_3{}^-$, 29477-05-2; $Co(CO)_3PBu_3{}^-PPN^+$, 118400-44-5; $Co_2(CO)_6(PPh_3)_2$, 10170-27-1; $Co_2(CO)_6(PBu_3)_2$, 14911-28-5; $Co_2(CO)_6(PPh_3)(PBu_3)$, 118400-48-9; $Co_2(CO)_8$, 10210-68-1; $Co(CO)_3(PPh_3)_2{}^+BF_4{}^-$, 118400-45-6; $Na^+Co(CO)_4{}^-$, 14878-28-5; $Co_2(CO)_6[P(p\text{-}tol)_3]_2$, 118400-47-8; $[Co(CO)_3(PBu_3)_2{}^+][Co(CO)_4{}^-]$, 15157-80-9; $[Co(CO)_3(PBu_3)_2{}^+][Co(CO)_3PBu_3{}^-]$, 118400-46-7; $Co(CO)_3(PEt_3)_2{}^+$, 52691-20-0; $Co(CO)_3(PPh_2Me)_2{}^+$, 55906-70-2; $Co(CO)_3(PPhMe_2)_2{}^+$, 87564-75-8; $Co_2(CO)_6(PPh_2Me)_2$, 31224-11-0; $Co_2(CO)_6(PPhMe_2)_2$, 21407-17-0; $Co(CO)_3PEt_3{}^-$, 82555-87-1; $Co(CO)_3PPh_2Me^-$, 62390-44-7; $Co(CO)_3PPhMe_2{}^-$, 82555-88-2; $Co(CO)_3P(p\text{-}tol)_3{}^-$, 118473-71-5; $[Co(CO)_3(PPh_3)_2{}^+][Co(CO)_4{}^-]$, 14243-08-4.

---

(74) Lau, W.; Huffman, J. C.; Kochi, J. K. *Organometallics* **1982**, *1*, 155.

(75) For details of the DPSC method, see: Bard, A. J.; Faulkner, L. R. p. 181 in ref 62d. $|i_r/i_f| = {}^1/_2(1 - 0.5^{1/2}) = 0.1465$.